journal of the international meteor organization

WGN

44:4
august 2016

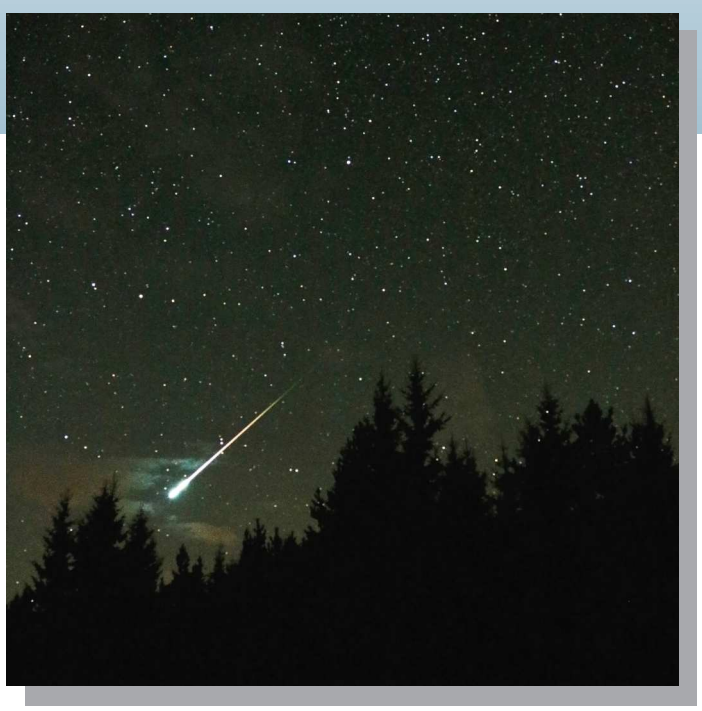

Quadrantids 2016 observed visually, by video and by radio
Discovery of the September Epsilon Draconids
February–March video meteors

ISSN 1016-3115

WGN Vol. 44, No. 4, August 2016, pp. 99 – 126

Administrative

Meteor science

Preliminary results

Front cover photo

Perseid fireball during the annual summer school at National Astronomical Observatory Rozhen in Bulgaria on 2016 August 10 at $00^{\mathrm{h}}06^{\mathrm{m}}$ UT using Canon EOS 750D camera with 18-mm lens at $f/5.6$ and 30 s exposure at ISO 6400. Image courtesy: Viktoria Mircheva.

Writing for WGN

This Journal welcomes papers submitted for publication. All papers are reviewed for scientific content, and edited for English and style. Instructions for authors can be found in WGN **31:4**, 124–128, and at `http://www.imo.net/docs/writingforwgn.pdf` .

Copyright

Legal address

International Meteor Organization, Jozef Mattheessensstraat 60, 2540 Hove, Belgium.

In Memoriam: Ichiro Hasegawa (1928 – 2016)

Masayoshi Ueda[1]

Received 2016 August 30

Ichiro Hasegawa, a long time researcher on meteors and comets, passed away May 1, 2016 in Kobe, Japan. He was born in Nishinomiya, Hyogo prefecture January 23, 1928. He married Michiko in 1960 and their first son was born in 1962 and the second child in 1963. He had wide interests and worked in extensive fields; ancient astronomy, celestial mechanics, comets, meteors and the direction of amateurs.

Hasegawa researched historical records of China, Korea and Japan between 1800 BC and 1862 AD and compiled a list of ancient meteor showers (Imoto & Hasegawa, 1958). He collected ancient astronomical records and calculated the orbits of 38 bright comets between 146 BC and 1557 AD (Hasegawa, 1979).

Hasegawa investigated celestial mathematics and calculated the radiants from comets (Hasegawa, 1958; revised 1985). He re-examined the calculation methods later and published the new list of cometary meteor radiants (Hasegawa, 1990). His predictions co-incide well with observations and many researchers have a high regard for it.

He published 'Distribution of the Aphelia of Long-Period Comets' in 1976 (Hasegawa, 1976a) and took his degree of Sc. D. from Kyoto University. He was a professor of Otemae University.

He calculated the predicted radiants from near Earth asteroids (Hasegawa et al., 1992) and added the prediction of the new NEOs (Near Earth Objects). We have paid attention to his notices and carefully watched them.

Hasegawa strove to instruct amateurs, publishing his books on celestial mechanics (e.g. Hasegawa, 1976b). This book has played important roles for Japanese amateurs, because it introduced us to the measurement of meteors on films and to the determination of meteor orbits. The author observed the re-entry of HAYABUSA, on 2010 June 13 at $13^{h}51^{m}$ (UT), from triple video stations in the Australian desert with Shiba, Y. and Yamamoto,

[1]43-2 Asuka Habikino-shi Osaka, 583-0842, Japan. The Nippon Meteor Society (NMS). Email: ueda@meteor.chicappa.jp

Figure 1 – Dr. Ichiro Hasegawa at his home in 2014.

M. We used the formulae of Hasegawa's 1976 book for determining its trajectory in the Earth's atmosphere precisely and the results give valuable information on an artificial meteor phenomenon (Ueda et al., 2011).

He had been the president of the Nippon Meteor Society and attended its annual meeting for giving strict and constructive criticism in order to support their studies. He has worked also for the Oriental Astronomical Association (OAA) as a director.

Hasegawa has looked upon the private study group (Juso-juku) since 2004 each month and guided the members to read new meteor papers. Most recently, he introduced and commented on the study on the sporadic meteor sources by video observations (Jakšová et al., 2015).

He has been a special person in celestial mechanics, meteor and comet science and ancient astronomy. We who knew him – I myself owe my meteor orbit calculations seriously to him – miss him deeply. We feel as we are sheep not having a shepherd.

Selected Bibliography

Hasegawa I. (1958, revised 1985). *Documentation des Observateurs*, volume 11. Nos. 1, 4, 8 and 11.

Hasegawa I. (1976a). "Distribution of the aphelia of long-period comets". *Publ. Astron. Soc. Japan*, **28**, 259–276.

Hasegawa I. (1976b). "Orbit calculation and physics of meteors". (in Japanese, a copy of holograph book).

Hasegawa I. (1979). "Orbits of ancient and medieval comets". *Publ. Astron. Soc. Japan*, **31**, 257–270.

Hasegawa I. (1990). "Predictions of the meteor radiant point associated with a comet". *Publ. Astron. Soc. Japan*, **42**, 175–186.

Hasegawa I., Ueyama Y., and Ohtsuka K. (1992). "Predictions of the meteor radiant point associated with an Earth-approaching minor planet". *Publ. Astron. Soc. Japan*, **44**, 45–54.

Imoto S. and Hasegawa I. (1958). "Historical records of meteor showers in China, Korea, and Japan". *Smithsonian Contributions to Astrophysics*, **2**, 131–144.

Jakšová I., Porubčan V., and Klačka J. (2015). "Structure and sources of the sporadic meteor background from video observations". *Publ. Astron. Soc. Japan*, **67:5**, 99(1–7).

Ueda M., Shiba Y., Yamamoto M., Fujita K., Watanabe J., Sato M., Abe S., Kakinami Y., Uehara S., Okamoto S., Fujiwara Y., and Tanabe T. (2011). "Trajectory of HAYABUSA reentry determined from multisite TV observations". *Publ. Astron. Soc. Japan*, **63:5**, 947–953.

IMO bibcode WGN-444-ueda-hasegawa NASA-ADS bibcode 2016JIMO...44...99U

Meteor science

Quadrantids 2016: observations of a short pre-maximum peak

Jürgen Rendtel[1,2], *Hiroshi Ogawa*[1,3] *and Hirofumi Sugimoto*[1,4]

The Quadrantid meteoroid stream is known to show variations between annual returns as well as signs of mass sorting along the cross section. Only a little modelling of the stream has been published. For 2016, a possible short flux enhancement a few hours before the main peak of the shower was announced. Here we present results obtained from two independent optical observation samples. The data strongly support the presence of the predicted feature at $\lambda_\odot = 282\,^\circ\!.884 \pm 0\,^\circ\!.010$ showing an increase by about 50 percent of the visual ZHR and about 25 percent of the video meteor flux compared to the neighbouring values. The width of the peak is of the order of 30 minutes. The population index profile indicates that the meteoroids are not different in size distribution form the surrounding stream. A similar narrow increase by about 50 percent is found in radio forward scatter data at $\lambda_\odot = 282\,^\circ\!.748 \pm 0\,^\circ\!.010$. This is $0\,^\circ\!.14$ or 3.4 hours earlier than the peak of the optical meteors and may be explained as a mass sorting effect in this part of the stream.

Received 2016 July 7

1 Introduction

The Quadrantids (010 QUA) is one of the three strongest annual meteor showers. It is effectively observable only from the northern hemisphere. Only the hours after about local midnight provide suitable radiant heights. The shower peak is of relatively short duration: the full width at half-maximum of the ZHR profile is about 14 hours. The often quoted maximum position at $\lambda_\odot = 283\,^\circ\!.15 \pm 0\,^\circ\!.04$ for visual meteors is based on the best-observed return of the shower in 1992 (Rendtel et al., 1993). Some complexity is added from the mass segregation observed within the stream. A relation between the meteor magnitude and the peak position has been derived by Hughes & Taylor (1977). A more recent study of the Quadrantid radar peak (magnitude +7.7; Brown et al., 1998) shows the peak at $283\,^\circ\!.08 \pm 0\,^\circ\!.08$, i.e. very close to the optical peak and not following the above mentioned relation. The position of the optical peak itself (approximately magnitude +3) also slightly varies from one return to another by a few hours (Table 1).

It is also known that the activity of the shower expressed as ZHR varies considerably by a factor of 2 or more (Table 1) between different returns of the shower in both the optical and radio meteor range.

In Table 1 we compiled all positions of the optical (visual) Quadrantid main peak available which are covered by data series around the peak between 1987 and 2016. Note that the ZHRs from the IMO live graphs have been calculated with a fixed $r = 2.1$. However, this has no effect on the shape and position of the peak. The effect of the rate level is negligible too, as the available magnitude data indicate a stable value of r very close to the assumed figure. Table 1 also lists the same information for the radio forward scatter data collected and analysed in the International Project for Radio Meteor Observation (Ogawa et al., 2004). The activity index gives a relative strength of the maximum (see section 3.4).

Currently, two objects are identified as parents of the stream: Comet 96P/Machholz and the minor planet 2003 EH_1 (see Wiegert & Brown, 2005, for a summary). Recent modelling hints at a very low age of the stream: it may be between a few thousand years (Jenniskens et al., 1997) or a few hundred years (Abedin et al., 2015). Attempts to predict the activity level have been made, but with limited success, probably due to the complex structure of the stream. A series of modelled Quadrantid meteoroid stream cross sections calculated by Vaubaillon from meteoroid ejection from 2003 EH_1 in 1491 only are given in Jenniskens (2006) on page 375 (Figure 20.17).

The 2016 Meteor Shower Calendar of the IMO (Rendtel, 2015) quoted a possible rate enhancement between January 3, 22^hUT and January 4, 02^hUT ($282\,^\circ\!.74 - 282\,^\circ\!.91$ solar longitude). This is about 10–6 hours before the anticipated regular peak time, within the ascending branch of the Quadrantid activity profile. No information was given regarding the expected density or a specific size distribution.

2 Quadrantid observations in 2016

During the entire Quadrantid activity period of the Quadrantids between 2015 December 28 and 2016 January 12, we received data from **38 visual observers** from 12 countries, comprising a total sample of 835 Quadrantids reported in 133 intervals, via the online form on the IMO website:

Stephen Bedingfield, Canada; Orlando Benítez Sanchez, Spain; David Buzgo, Serbia; Yisheng Gong, China; Karoly Jonas, Hungary; Katsuyuki Kobayashi, Japan; Ralf Koschack, Germany; Richard Kramer, United States; Artem Mirgorod, Ukraine; Sirko Molau, Germany; Maciek Myszkiewicz, Poland; Shangyi Ning, China; Pedro Perez Corujo, Spain; Yunyao Que, China; Ina Rendtel, Germany; Jürgen Rendtel, Germany;

[1]International Meteor Organization (IMO)
[2]Leibniz-Institut für Astrophysik Potsdam (AIP), An der Sternwarte 16, 14482 Potsdam, Germany. Email: jrendtel@aip.de
[3]The Nippon Meteor Society, Sakashita 3-12-12-502, Itabashi, Tokyo, 174-0043, Japan. Email: h-ogawa@amro-net.jp
[4]The Nippon Meteor Society, Sennincho 1-6-15, Hachioji, Tokyo, 193-0835, Japan. Email: h-sugimoto@amro-net.jp

Table 1 – Quadrantid peaks observed visually and peak data from radio observations compiled by the "International Project for Radio Meteor Observation" including contributions from observers in 8 – 25 countries (different in each year). The peak position is estimated from a Lorentz profile. The activity index calculated according to Miyao & Ogawa (2004) describes a relative strength of the peak.

	Visual Quadrantid peak data			Quadrantid peak radio data		
Year	Peak $\lambda_\odot$	ZHR	Reference, comments	Peak $\lambda_\odot$	Activity	Comments
1987	$283^\circ.08 \pm 0.12$	140 ± 10	Rendtel et al., 1993, Fig. 10			
1989	$283^\circ.30 \pm 0.15$	70 ± 10	Rendtel et al., 1993, Fig. 11			
1990	$283^\circ.30 \pm 0.08$	78 ± 10	Rendtel et al., 1993, Fig. 12			
1992	$283^\circ.15 \pm 0.10$	145 ± 5	Rendtel et al., 1993			
1995	$283^\circ.35 \pm 0.20$	110 ± 15	Jenniskens et al., 1997, Fig. 6			
1997	$283^\circ.10 \pm 0.10$	93 ± 15	Brown et al., 1998, Fig. 12			
2001				$283^\circ.320$	6.4 ± 0.8	late peak $283^\circ.575, 4.8 \pm 2.0$
2002				$283^\circ.310$	9.2 ± 0.4	
2003				$283^\circ.010$	6.4 ± 1.7	late peak $283^\circ.561, 3.4 \pm 0.5$
2004				$283^\circ.126$	6.7 ± 1.7	
2005				$283^\circ.213$	6.0 ± 0.3	late peak $283^\circ.45, 4.5 \pm 0.5$
2006				$283^\circ.167$	4.9 ± 1.0	late peak $283^\circ.545, 2.5 \pm 0.1$
2007				$283^\circ.280$	4.6 ± 0.6	
2008	$283^\circ.26 \pm 0.04$	82 ± 8	live graph	$283^\circ.152$	3.9 ± 1.3	
2009	$283^\circ.15 \pm 0.04$	160 ± 18	live graph	$283^\circ.349$	4.6 ± 1.2	no clear peak
2010				$283^\circ.051$	3.6 ± 0.8	
2011	$283^\circ.24 \pm 0.05$	74 ± 4	live graph; high ZHR at $283^\circ.05$	$282^\circ.875$	5.1 ± 0.9	complex structure
2012	$283^\circ.08 \pm 0.06$	82 ± 5	live graph	$283^\circ.20$	4.2 ± 0.5	double peak? ($283^\circ.0, 283^\circ.46$)
2013	$283^\circ.03 \pm 0.08$	135 ± 40	live graph	$283^\circ.10$	4.8 ± 0.5	double peak? ($282^\circ.95, 283^\circ.33$)
2014	$283^\circ.18 \pm 0.05$	245 ± 21	live graph	$283^\circ.112$	8.3 ± 0.4	
2015				$283^\circ.05$	2.4 ± 0.3	
2016				$283^\circ.056$	7.4 ± 1.5	

Terrence Ross, United States; Mikiya Sato, Japan; Branislav Savic, Serbia; Hideki Seo, Japan; Fangzheng Shi, China; Ivan Stankovic, Serbia; Ziwei Su, China; Istvan Tepliczky, Hungary; Kazumi Terakubo, Japan; Snezana Todorovic, Serbia; Shigeo Uchiyama, Japan; Andras Uhrin, Hungary; Valentin Velkov, Bulgaria; Xiaoyu Wang, China; Roland Winkler, Germany; Hong Yan, China; Jinye Yang, China; Jiaying Yang, China; Takao Yoshimura, Japan; Paul Zeller, United States; Yinghua Zhang, China; Zixue Zhou, China

For the present analysis we were looking into details shortly before the main peak which is well covered with data. A continuous series is available for the period between January 3, 20^h UT and January 4, 08^h UT. The start and end of this period are less covered, mostly due to the geographical distribution of the observers. The end is caused by the "Atlantic gap". However, the sample is sufficient to look into the period including the predicted rate peculiarity, but we do not have sufficient data to cover the main peak period. The series enters the gap immediately before the peak activity of the Quadrantids occurs.

Remember that the radiant reaches its lowest point around 20^h local time. At a geographical latitude of 50° N, the radiant climbs above 20° elevation at 0^h10^m local time, while that will happen at 2^h20^m local at a latitude of 30° N. The window opens wider for observers further north: already at 54° N the radiant has the same elevation more than an hour earlier than at 50° N.

The **cameras of the IMO Video Meteor Network** also covered the respective time interval, but interrupted by the "Atlantic gap" in the same manner as the visual series. However, the large number of active cameras allows us to select shorter bins than the limited visual sample.

Another data set is compiled from **world-wide forward scatter radio meteor counts.** In 2003, the international project for combination of such data was presented at the IMC (Ogawa et al., 2004). It produces meteor shower activity profiles regularly, expressed as a radio ZHR:
`www5f.biglobe.ne.jp/~hro/Flash/2016/QUA/`
(see section 3.4).

3 2016 observational results

3.1 Population index profile

The population index r is an essential quantity for the appropriate correction of individual count data to calculate the ZHR and later the flux. It is known that the value of r can significantly vary along the Earth's path through a meteoroid stream. Thus the determination of r is the first step in our analysis despite the fact that the size of the visual sample is not large enough to detect fine structures. Our main goal is to check whether we can detect any peculiarity in the interval of the possible rate enhancement. A deviation from the neighbouring intervals could indicate another dust composition. Video data have been used to determine r values for short intervals only for the Perseids 2015 (Molau et al., 2015).

The highest possible resolution for the population index profile obtained from the visual data is shown in Figure 1; the values are given in Table 2. The available data set allows us to calculate roughly one value each 1.25 hours. Depending on the duration of a possi-

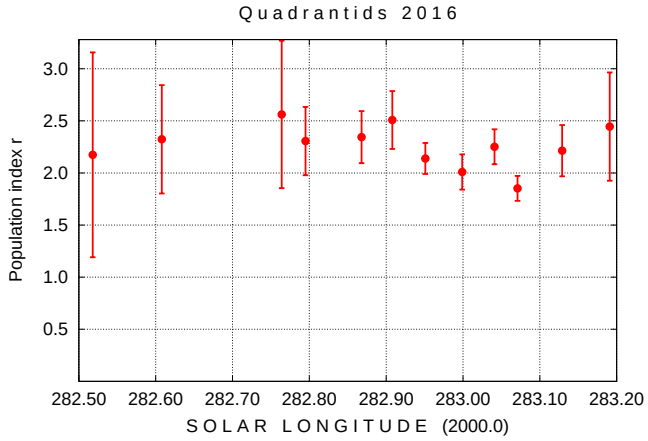

Figure 1 – Profile of the population index r of the 2016 Quadrantids – all values listed in Table 2 including the start of the maximum night until the end of the series in the European morning hours.

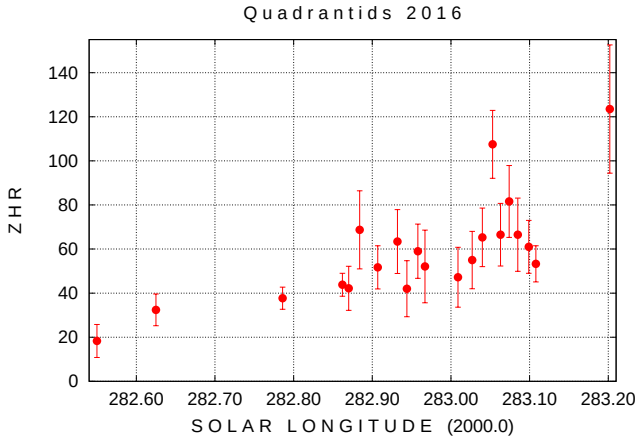

Figure 2 – Profile of the (visual) ZHR of the 2016 Quadrantid maximum. The numerical values are listed in Table 3.

Table 2 – The population index r derived from the visual data of the 2016 Quadrantid return during the ascending activity period before the main rate peak. Also listed are the number of intervals and number of Quadrantids used in the calculation.

$\lambda_\odot$	Popul. index r	Int.	QUA
282.518	2.17±0.98	4	13
282.608	2.32±0.52	3	24
282.764	2.56±0.71	2	26
282.795	2.31±0.33	4	48
282.868	2.34±0.25	5	81
282.908	2.51±0.28	5	89
282.951	2.14±0.15	11	151
282.999	2.01±0.17	6	84
283.041	2.25±0.17	7	133
283.071	1.85±0.12	6	107
283.129	2.21±0.25	5	65
283.191	2.44±0.52	2	31

ble passage of the Earth through a stream feature, we might just expect a minor change as additional meteoroids comprise only a small additional portion to the average Quadrantid stream. The profile shows no pattern whatsoever, which could be attributed to an additional component – if something occurs, it is within the error margins.

The lower r at 283.°00, i.e. about 4 hours before the expected peak position, may be a hint at the often described mass segregation, indicating that we find a slightly higher portion of brighter Quadrantids before the actual peak is reached. The possible effect of the increasing radiant elevation towards the morning on the meteoroid trajectories in the atmosphere has been discussed by Bellot Rubio (1994). This is the case in our current data set as well which to some extent repeats the situation analysed by Bellot Rubio, although the observers contributing to the 2016 sample were located at more scattered sites and thus reducing the effect. Hence the values of r calculated with low radiant positions at a few sites have less influence and the corrections are well below the values of $\Delta r = +0.14$ at 40° radiant elevation and +0.05 at 60° radiant elevation (Bellot Rubio, 1994).

The 2016 data does not allow us to check the further shape of the r-profile as the number of reported meteors becomes too small. There is one further – and indeed higher – value calculated at $\lambda_\odot = 283.°191$, giving $r = 2.44 \pm 0.52$ but it is based only on two intervals including 31 Quadrantids (see Table 2). However, the value and position are identical to the values found at the respective position in the well analysed 1992 profile.

3.2 Visual ZHR profile

Using the r-profile, we calculated the ZHRs. Like with the population index profile, we have to adjust the interval lengths such that we do not lose temporal resolution but to ensure that the sample per bin is not too small. Here we shifted a 1-hour interval by 20-minute steps which is a slight oversampling and thus at the limit of the given data set. The result is shown in Figure 2 with the values listed in Table 3. At the end of the interval the ZHR increases towards the main peak position which occurs too late to be covered by European observers and therefore falls in the "Atlantic gap".

In order to check for possible rate anomalies, we have a close look into the interval indicated by the prediction, using all data from $\lambda_\odot = 282.°78$ to 282.°98. The values in the hours before (1 hour corresponds to 0.°042 in solar longitude) seem to show mainly scatter. There are two ZHR values which are higher than in the neighbouring intervals. The intervals are centered at $\lambda_\odot = 282.°884$ and 283.°053. The latter is already quite close to the main peak. If we had just this one profile, we would ignore such enhancements as their significance is quite low (seen the error margins and the rather small sample). This time we do have more data at hand.

3.3 Video flux data

Here we use the possibilities provided by the webpage `meteorflux.io` which allows us to calculate flux data and to adjust several parameters interactively. We ap-

Table 3 – Quadrantid ZHR values calculated for the interval before the main peak discussed in this paper, using the r-profile obtained first.

$\lambda_\odot$	ZHR	QUA
282.550	18.3± 7.5	5
282.625	32.4± 7.2	19
282.786	37.7± 5.0	55
282.862	43.8± 5.2	69
282.870	42.2±10.0	17
282.884	68.7±17.7	14
282.907	51.7± 9.8	27
282.932	63.4±14.5	18
282.944	42.0±12.7	10
282.958	59.0±12.3	22
282.967	52.1±16.5	9
283.009	47.2±13.6	11
283.027	55.0±13.0	17
283.040	65.3±13.3	23
283.053	107.5±15.4	48
283.063	66.5±14.2	21
283.074	81.6±16.3	24
283.085	66.5±16.6	15
283.099	61.0±12.0	25
283.108	53.3± 8.2	41
283.202	123.5±29.1	17

ply $r = 2.1$ as a constant value over the period. This is well within the range we calculated from the visual data before. Using $r = 2.3$ instead does not give a different result, particularly because we are looking for the shape rather than absolute values. A flux profile with higher temporal resolution is shown in the January 2016 video data analysis (Molau et al., 2016), also using $r = 2.1$ for the entire profile. Both the video flux data calculated for this analysis as well as the high resolution profile show enhanced flux in the interval at $\lambda_\odot = 282.^\circ884$ (Table 4 and Figure 3).

The high ZHR later in the visual profile at $\lambda_\odot = 283.^\circ053$ seems to occur also in the video meteor flux data represented by the last value which is of low significance due to the small sample at the end of the series. We assume that this feature belongs to the structure of the main peak as the ZHR and the flux start to rise after $\lambda_\odot = 283.^\circ0$ in both series obtained in the optical range.

3.4 Radio forward scatter data

The radio forward scatter meteor data define a general activity profile with a maximum activity of 7.4 ± 1.5 at $\lambda_\odot = 283.^\circ14$ corresponding to January 4, $07^{\mathrm{h}}30^{\mathrm{m}}$ UT with a FWHM of 13 hours, derived from the fitted profile (Figure 4). The later estimate of the peak ZHR of 160 for the 2016 maximum is calculated using a least squares fit between the activity level and the visual ZHR over several maxima (Ogawa et al., 2004). The analysis of the forward scatter meteor counts works in two steps. First, we define a quantity CHR_r which gives the difference between the total number and the number of sporadic meteors. The sporadic meteor number is calculated from the data of the past 14 days. Then, the ZHR is calculated: ZHR_r = CHR_r $\times 1/\sin(h)$ with h the radiant elevation, excluding intervals with $h < 20°$.

Table 4 – Flux of the Quadrantids 2016 calculated from video data collected by the IMO Video Meteor Network, using `meteorflux.io` (bin duration 15 min – 2.0 hours, 40 meteors per bin, minimum collecting area 25000 km^2). The last value is based on very few meteors only and has been added to show the rise towards the main peak.

$\lambda_\odot$	Flux 10^{-3} km^{-2} h^{-1}	QUA
282.774	9.2±1.4	37
282.802	10.0±1.5	40
282.826	9.3±1.4	37
282.847	11.1±1.7	44
282.862	13.0±2.0	52
282.873	13.8±2.1	55
282.884	21.3±2.6	85
282.895	14.0±2.0	55
282.906	15.0±2.1	60
282.917	17.7±2.2	71
282.928	14.8±2.0	59
282.939	14.2±1.9	56
282.950	15.9±2.0	63
282.961	15.5±2.0	62
282.972	19.4±2.3	77
282.983	16.7±2.1	67
282.994	17.3±2.0	69
283.005	15.5±1.9	61
283.016	19.8±2.1	79
283.027	22.4±2.4	89
283.038	23.5±2.4	94
283.049	18.3±2.4	73
283.070	24.2±6.6	13

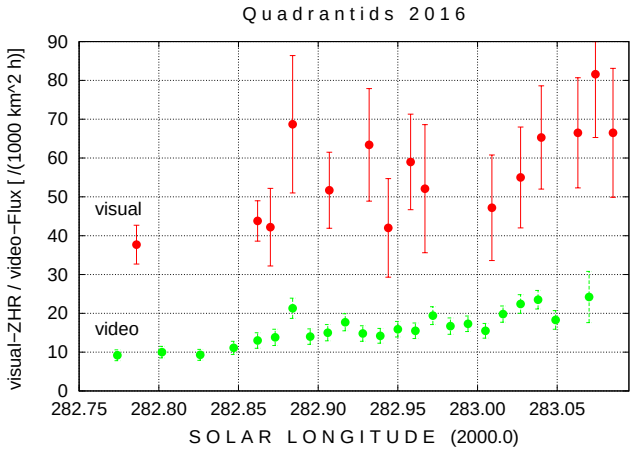

Figure 3 – Profiles of the (visual) ZHR and the (video) meteor flux of the 2016 Quadrantids for the period around the rate enhancement discussed in section 3.2. The respective values are listed in Tables 3 and 4.

The activity profile obtained from forward scatter data (Figure 4) shows the ascent towards the main peak starting near $\lambda_\odot = 282.^\circ85$. Since the peak is located at $\lambda_\odot = 283.^\circ14$, the width of the Quadrantid maximum seems to be wider for faint meteors than for optical meteors. This indicates that the enhancement at $\lambda_\odot =$

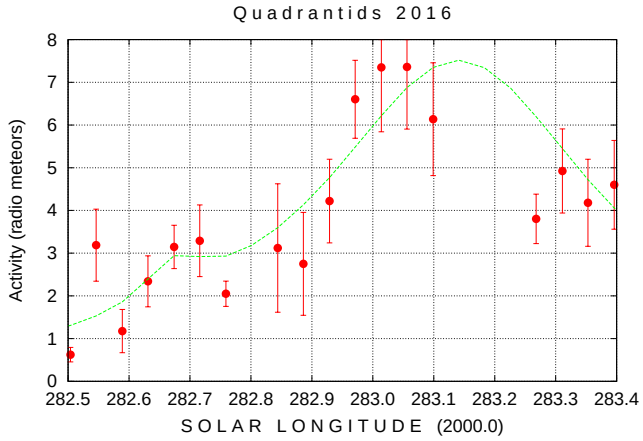

Figure 4 – Profile of the radio forward scatter meteor activity of the 2016 Quadrantids for the entire maximum period. The line shows a Lorentz profile of the maximum period and was calculated according to Jenniskens et al. (1998).

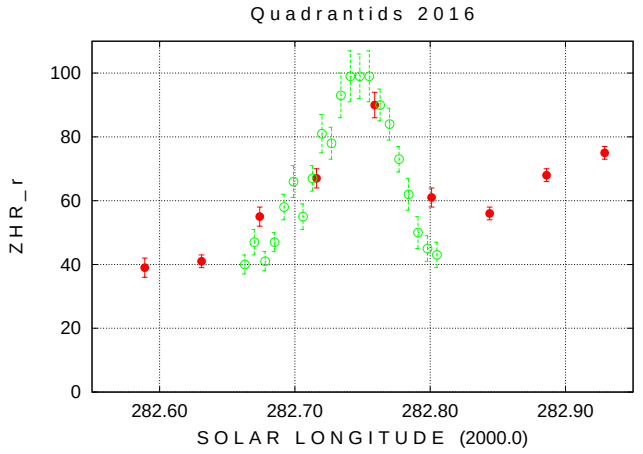

Figure 5 – Profile of the radio forward scatter ZHR_r showing a short-lived peak at $\lambda_\odot = 282\,^\circ\!.748$. The general profile is based on 1-hour data (dots), while the peak profile is defined by 10-minute data (circles).

283 °.053 discussed in sections 3.2 and 3.3 is indeed part of the main Quadrantid peak.

For the detailed analysis of the 2016 Quadrantid activity during the ascending branch we combine ZHR_r-data with 1-hour timesteps (29 observing sites in ten countries worldwide) with 10-minute steps derived from four observing sites only in Japan (Figure 5). The high temporal resolution data show a small peak at $\lambda_\odot = 282\,^\circ\!.748$, corresponding to January 3, $22^{\rm h}15^{\rm m}$ UT with a FWHM of 2.5 hours and a ZHR_r of 99 ± 8.

The ZHR_r-profile shown in Figure 5 clearly shows a significant peak at $\lambda_\odot = 282\,^\circ\!.748 \pm 0\,^\circ\!.010$, i.e. shortly before the optically observed peaks (see Table 5). This obvious difference in the time hints at a different mass range of the meteoroids responsible for the peak in the radio region (fainter meteors, perhaps +6 magnitude) and the optical range (+3 magnitude). The difference is 0 °.14 in solar longitude, or 3.4 hours. Checking the ZHR and flux values, we do not find an enhancement in these data at the time of the radio rate peak.

Table 5 – ZHR_r-values of the Quadrantids 2016 calculated from forward scatter meteor data collected by the international project for radio meteor observation. The top section gives the 1-hour data, the bottom section lists the 10-minute values as explained in the text.

$\lambda_\odot$	ZHR_r (1 hour)
282.504	30±3
282.546	35±3
282.589	39±3
282.631	41±2
282.674	55±3
282.716	67±3
282.759	90±4
282.801	61±3
282.844	56±2
282.886	68±2
282.929	75±2
$\lambda_\odot$	ZHR_r (10 min)
282.663	40±3
282.670	47±4
282.678	41±3
282.685	47±3
282.692	58±4
282.699	66±5
282.706	55±4
282.713	67±4
282.720	81±6
282.727	78±5
282.734	93±7
282.741	99±8
282.748	99±7
282.755	99±8
282.763	90±5
282.770	84±5
282.777	73±4
282.784	62±5
282.791	50±5
282.798	45±4
282.805	43±4

3.5 Summary of 2016 Quadrantid data

In Figure 6, we show all profiles we obtained: the visual ZHR profile, the video flux profile with similar temporal resolution and the ZHR_r profile of radio meteors. Again, looking back into the profile of the population index r (Figure 1), there is no sign of a feature indicating a deviating magnitude distribution at the given position. So the obviously detected density enhancement at $282\,^\circ\!.884 \pm 0\,^\circ\!.008$, corresponding to $01^{\rm h}28^{\rm m}$ UT ±12 min seems to consist of meteoroids with essentially the same size distribution as the surrounding region of the stream.

4 Conclusions

Using independent data samples of the 2016 Quadrantids covering different magnitude ranges, we are able to detect very weak and narrow structures in the Quadran-

Table 6 – Positions of slightly enhanced ZHR/flux in the Quadrantid data in the night 2016 January 03–04.

Data sample	Minor peak	Time UT	FWHM
Radio ZHR	282.°748	22^h15^m	0.°10 (2.5h)
Visual ZHR	282.°884	01^h28^m	0.°02 (0.5h)
Video flux (this work)	282.°884	01^h28^m	0.°02 (0.5h)
Video flux (Molau et al., 2016)	282.°886	01^h30^m	0.°015 (0.3h)

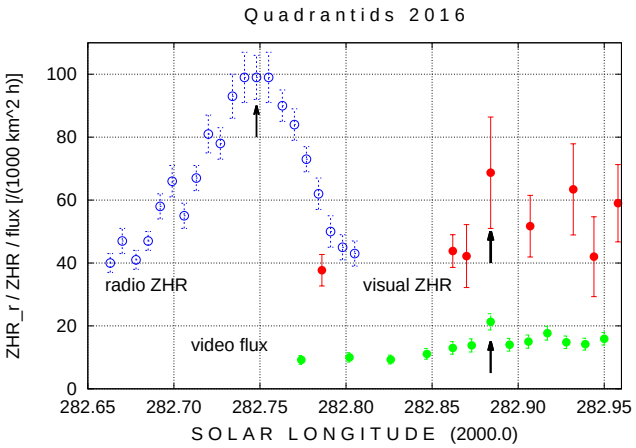

Figure 6 – Profiles of the ZHR and flux of the 2016 Quadrantids in the period discussed in this work. Dots show optical (visual and video) data, circles are used for the radio ZHR_r. The arrows indicate the peak positions in the different data sets.

tid meteoroid stream at $282.°884 \pm 0.°008$ in the optical range (meteor magnitude +3) and at $\lambda_\odot = 282.°748 \pm 0.°010$ in the radio meteor range (meteor magnitude +6). A later short ZHR and flux enhancement at $\lambda_\odot = 283.°053$ is attributed to the main peak of the Quadrantids. The ascent starts at $\lambda_\odot = 282.°85$ in the radio forward scatter meteor data and at $\lambda_\odot = 283.°0$ in the optical data. Since the peak times coincide close to $\lambda_\odot = 283.°15$, this indicates a wider profile for fainter Quadrantids. As the optical data only cover the ascending branch, we may estimate the FWHM of the optical peak to be 0.°30 while the radio meteor peak may have a FWHM close to 0.°8.

A similar case of a short rate and flux enhancement has been found within the Perseid stream in August 2015 (Molau et al., 2015) using independent video and visual data samples. Careful analyses of observational data obtained by different techniques enable us to find structures in meteoroid streams which seem to be close to the detection limit but can be verified by a combined sample. We suggest that the observational results are used to adjust parameters introduced in the stream modelling which led to the prediction of the rate/flux enhancement for the 2016 return of the Quadrantids. If we treat the two peaks in the optical and radio meteor ranges as real structures of the stream, the modelling needs to consider the shift of about 3 hours in the peak timing for different mass ranges and the different widths of the peak given in Table 6.

Although the Quadrantid shower belongs to the strongest meteor showers with annual high rates, the amount of data seems not sufficient for a comprehensive long-term study of the meteoroid distribution along the stream's orbit. Some results have been summarized in 1992 (Rendtel et al., 1993) and also for 1997 (combining optical and radar data: Brown et al., 1998) as well as in our Table 1. All profiles of the population index r or the mass index s around the main peak show roughly a U-shape with a minimum shortly before $\lambda_\odot = 283°$ and a subsequent rise immediately after that. The late peak found in radio data on several returns (see Table 1) located near $\lambda_\odot = 283.°5$ is not present in the optical data and is perhaps also a specific feature due to mass separation and maybe helpful to set stream model parameters.

Acknowledgement

Personal note (JR): one reason to start analysing the relatively small sample of the visual 2016 Quadrantids was a tour together with Sirko Molau in the night 3/4 January to observe the early part of the ascending activity under clear skies, −15°C and strong wind over five hours. The result shown here, including other samples, is satisfying and motivating for further campaigns to check possible minor activity of meteor showers.

References

Abedin A., Spurný P., Wiegert P., Pokorný P., Borovička J., and Brown P. (2015). "On the age and formation mechanism of the core of the Quadrantid meteoroid stream". *Icarus*, **261**, 100–117.

Bellot Rubio L. R. (1994). "Dependence of the population index on the radiant zenithal distance". *WGN, Journal of the IMO*, **22:1**, 13–26.

Brown P., Hocking W. K., Jones J., and Rendtel J. (1998). "Observations of the Geminids and Quadrantids using a stratosphere-troposphere radar". *MNRAS*, **295**, 847–859.

Hughes D. W. and Taylor I. W. (1977). "Observations of overdense Quadrantid radio meteors and the variation of the position of stream maxima with meteor magnitude". *MNRAS*, **181**, 517–526.

Jenniskens P. (2006). *Meteor Showers and Their Parent Comets*. Cambridge University Press.

Jenniskens P., Betlem H., de Lignie M., Langbroek M., and van Vliet M. (1997). "Meteor stream activity: V. The Quadrantids, a very young stream". *Astron. Astrophys.*, **327**, 1242–1252.

Jenniskens P., Crawford C., Butow S. J., Nugent D., Koop M., Holman D., Houston J., Jobse K., Kronk G., and Beatty K. (1998). "Lorentz shaped comet dust trail cross section from new hybrid visual and video meteor counting technique – implications for future Leonid storm encounters". *Earth, Moon, and Planets*, **82**, 191–208.

Miyao K. and Ogawa H. (2004). "Research into the characteristics of meteor showers from multi-frequency radio observations". In Triglav-Čekada M. and Trayner C., editors, *Proceedings of the International Meteor Conference, Bollmannsruh, Germany, September 19-21, 2003*. IMO, pages 81–89.

Molau S., Crivello S., Goncalves R., Saraiva C., Stomeo E., and Kac J. (2015). "Results of the IMO Video Meteor Network – August 2015". *WGN, Journal of the IMO*, **43:6**, 188–194.

Molau S., Crivello S., Goncalves R., Saraiva C., Stomeo E., and Kac J. (2016). "Results of the IMO Video Meteor Network – January 2016". *WGN, Journal of the IMO*, **44:3**, 92–97.

Ogawa H., Toyomasu S., Ohnishi K., Maegawa K., Amikura S., and Miyao K. (2004). "The international project for radio meteor observation 2001–2003". In Triglav-Čekada M. and Trayner C., editors, *Proceedings of the International Meteor Conference, Bollmannsruh, Germany, September 19-21, 2003*. IMO, pages 107–113.

Rendtel J. (2015). "2016 Meteor Shower Calendar". International Meteor Organization. IMO INFO(2-15).

Rendtel J., Koschack R., and Arlt R. (1993). "The 1992 Quadrantid meteor shower". *WGN, Journal of the IMO*, **21:3**, 97–109.

Wiegert P. and Brown P. (2005). "The Quadrantid meteoroid complex". *Icarus*, **179**, 139–157.

Handling Editor: David Asher

This paper has been typeset from a LaTeX file prepared by the authors.

A search for undiscovered meteor showers: discovery of the September epsilon Draconids

Roberto Gorelli[1]

The author has processed a sample of sporadic meteors observed by the European viDeo MeteOr Network Database (EDMOND), a European network of cameras, in order to search for the possible existence of still unknown periodic meteor showers. The research has found new showers and confirmed other recently discovered showers. This article illustrates the characteristics of one new discovered shower and the confirmation of two others discovered by other researchers.

Received 2016 July 24

1 Key assumptions

The present work introduces a new concept: the "halo meteors", or meteors forming a cloud enveloping the torus of the meteor shower: these meteors characterize having slightly different orbital parameters compared to those typical of meteors being part of the shower, but similar enough to be considered originating from the same parent body.

2 Introduction

The meteor showers recently discovered through camera observations induced the author to examine those classified as "sporadic": 12 664 meteor orbits observed between 2009 August 10 and 2012 August 29 and classified at the time as sporadic have been analyzed by specialized software programs.

Every celestial body from the Solar System is defined by 7 orbital elements; among these, the semi-major axis (a) and the perihelion distance (q) determine the size of the orbit, the eccentricity (e) the orbit shape, the ascending node longitude, the pericentre argument and the inclination (Ω, ω and i) determine the orientation of its orbital plane in relation to the Earth. The seventh (T) shows the perihelion passage time.

Many factors must be taken in consideration to calculate a meteor orbit from the Earth, such as the Earth's gravity, the variations of the light refraction at different azimuths, the atmosphere friction and others. The incomplete or incorrect knowledge of these elements can totally or partially invalidate the results of optical observations made by cameras or very high light sensitivity cameras.

The main cause of unreliability is due to the limited length – usually no longer than 100 km – of the meteor's trajectory in Earth's atmosphere. In fact, the segment we observe is only a small fraction of the meteor orbit. This introduces a non negligible uncertainty in the calculation of the orbital elements; by analogy, at least several days of observations are needed to calculate the orbit of a periodic comet with a 5 AU semi-major axis. Very long period comets require considerably longer periods of observation. To this problem should be added to the meteor deceleration in the atmosphere: in principle, knowing the shape and, particularly, the density of the meteoroid, along with the atmospheric conditions at the time of the transit, we can calculate a relatively reliable meteor slowdown value. Such parameters, however, are generally unknown. These two factors – observational period and slowdown uncertainties – determine the geocentric and heliocentric velocity value which, in turn, lead to uncertainty in the meteoric orbit length.

For these reasons, although the orbital elements of the studied meteors – relative to the orientations of their orbital planes, compared to the Earth's orbit – have been considered reliable, geocentric and heliocentric velocities, and also the semi-major axis and eccentricity, have been considered potentially affected by systematic errors.

In the course of processing the results from this present work, it became necessary to create a new expression to describe a new concept: the "halo meteor". What is this? This term describes meteors that are midway between those that constitute the meteor shower and those regarded as sporadic. Why is this necessary? Because during the detailed work to differentiate between true sporadic meteors and the meteors that constitute the meteor showers being reported on, it became clear that there are meteors that are apparently linked to a meteor shower but whose D criterion values fall outside the normal range of the core members of that meteor shower. They cannot be considered to be core members of the meteor shower but we also cannot exclude them. They are the meteors that are shifting slowly, via gravitational perturbations and the Poynting-Robertson effect, from the meteor shower towards the sporadic background.

3 Procedure of the study

In order to discover the existence of still unknown showers, we started from the hypothesis that the individual orbital elements of meteors were uniformly distributed; that is, for every arbitrary unit of each orbital element there was an equal number of meteors. This working hypothesis does not reflect the reality, as statistical fluctuations, planetary perturbations and the same unknown showers produce values thickening or thinning of each orbital element, preventing the possible existence of this uniform distribution; concept so introduced only as an abstract point of departure.

In order to carry out the present work I utilized the orbital elements of 12 664 sporadic meteors recorded between years 2009 and 2012 and stored in the database

[1]Email: md6648@mclink.it

IMO bibcode WGN-444-gorelli-sed
NASA-ADS bibcode 2016JIMO...44..108G

EDMOND, a database of video meteor orbits compiled using data from European networks of meteor cameras (Kornoš et al., 2014a).

To find new showers we examined the orbital elements that determine the orientations of the meteor orbits with respect to the Earth's orbital plane. We started by inspecting the inclination and argument of the meteor's perihelion, dividing the 12 664 examined meteors into blocks (sets) of 10° tilt. Each of these blocks was then divided into sub blocks, 10° of perihelion argument, obtaining in all 648 sets (18 blocks of 10° tilt, each one correlated by 36 blocks, 10° perihelion arguments). Why divide the meteors into 10° sets? Because for almost all of the known meteor showers, individual orbital elements are dispersed in intervals of less than 10° and, also, the larger the blocks are, the greater is the risk of false showers. On the other hand, the use of smaller intervals sets could cause the researcher to miss the larger orbital interval showers.

As for the solar longitude – although this is generally considered one of the main criteria for the assignment of a meteor to a particular meteor shower – at the initiation of the research there are not yet any established strict criteria, as meteor shower durations range from a few hours (fractions of solar longitude degree), up to about 60 days (about 60° in solar longitude). The Author has restricted consideration of low inclination meteor sets to just those sharing from a few up to more than 30 degrees solar longitude, amounting to about 30 days, and – as for high inclination showers – only those not exceeding 10° dispersion were examined.

Each of the 648 initial sets was then divided into 20 subsets of 0.05 AU, resulting in a total of 12 960 subsets. The decision to divide the sets into 0.05 AU subsets, an arbitrarily chosen value, is due to the fact that the aphelia of meteors coming from already known meteor streams can be very different, while their perihelia values are very similar. The difference occurs because the meteoroids were mainly generated at the perihelion passage of the parent body and the vectors of the kinetic energy, received at the moment of the expulsion, ensure that, while the perihelion distance remains practically unchanged, the other orbital elements – in particular the eccentricity, the semi-major axis and consequently the aphelion – can be highly different from those of the parent body.

The meteors were then divided into files, each containing those included in a block of 10° tilt, to which meteors of 5° above and 5° below have been added, so as not to miss the showers across the two blocks. The meteors in each file have been organized by perihelion argument and divided into 10° sub blocks. The Author investigated the meteors sets included in 10° intervals of perihelion argument and removed the objects not falling in the same 0.05 AU interval of perihelion distance. Finally, those sets with less than 10 meteors were removed.

An hypothetical uniform distribution would result in an average value of 19.54 meteors per set, and 1.023 meteors for each subset. The reality, given random statistical fluctuations, could create sets from unrelated meteors, resulting in false showers. It was decided, therefore, to accept as possible showers only groups with 10 or more meteors, as this value allows a sufficient statistical significance for each of these groups. Therefore, the D criterion cannot be applied to sets consisting of less than 10 meteors (Klačka, 2000).

D criterion is a method used in Meteoritics to check membership of a meteor in a given shower: in fact one can speak of D criteria because, after the initial formulation of the principle, in 1963, by Southworth and Hawkins (D_{SH}), several variations have been formulated: in 1981 by Drummond (D_{D}), in 1993 by Jopek (D_{H}), Valsecchi and others (D_{N}), in 2008 by Jopek, Rudawska and Bartczak (D_{V}) and, finally, in 2008 by Jenniskens (D_{B}) (see summary in Jopek, 2011). All these versions consist in a mathematical equation giving rise to a common core; the terms of these versions differ one to the other, so that it can be possible – according to one or another – to emphasize different orbital elements. The choice of a version rather than another depends on the opinion of the individual researcher. The author of this work would have used the earlier variant of Southworth and Hawkins (D_{SH}), that gives much importance to the perihelion distance. Unfortunately, he did not find software for performing calculations; therefore he used the Drummond variant (D_{D}), that emphasizes the eccentricity (Welch, 2001; Langbroek, 2007).

This variant (D_{D}), tested on prograde meteor showers, reports links with a specific meteor shower with the value 0.08 for 50% of meteors, for 70% of the meteors with value 0.11 and for 90% of the meteors with value 0.18 ; for meteors coming from retrograde showers, it reports links for 50% of meteors with value 0.12, for 70% of meteors with value 0.18 and for 90% of meteors with value 0.28 (Galligan, 2001).

4 Results and discussion

The present work shows the first results of the research. Subsequent articles will show the remaining results: It should be noted that the showers considered below are not the only ones found in the sets examined, but are the ones that show the smallest dispersion in their orbital elements, while others, some of which are even more compact in the dispersion of the orbital elements, do not reach the limit of 10 meteors and – to be considered real showers – they must wait for future observations. Meteors sets forming new showers are presented and discussed below.

4.1 September epsilon Draconids (796 SED)

This shower comes from the study of 19 meteors: 12 belonging to the shower itself and 7 halo meteors. Orbital data for these meteors are shown in Table 1: as specified above, the perihelion and inclination argument are included in a less than 10° interval (Figures 1 and 2). The 12 meteors subjected to the Drummond criterion (D_{D}) were have values between 0.0191 and 0.0691, with an average value of 0.0464 (Table 2). On the basis of only the data of the present work there is a possibility

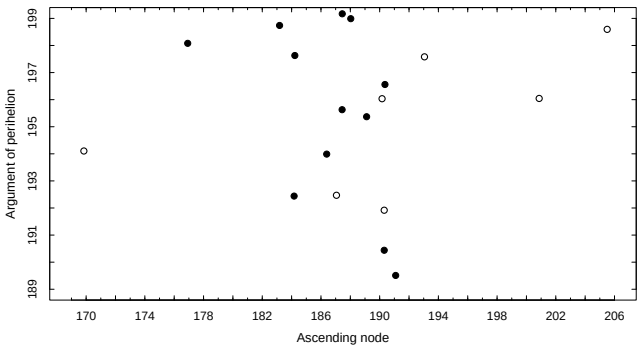

Figure 1 – The values of the ascending node and Argument of perihelion of September epsilon Draconids. The open circles represent halo meteors of the shower and were not utilized in the present work.

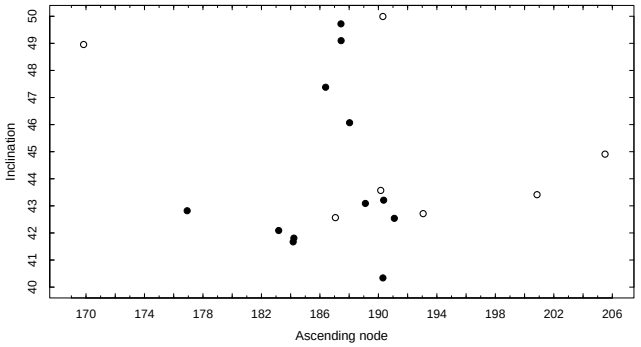

Figure 2 – The values of the ascending node and inclination of September epsilon Draconids. The open circles represent halo meteors of the shower and were not utilized in the present work.

of 5.1% that the shower does not exist and was only a chance occurrence ($p = 0.051$). The geocentric coordinates of the radiant of the meteors are presented in the Figure 3.

Key Features

The visibility period is between 176° and 192° of solar longitude, roughly corresponding to the period September 18 – October 5, or between 168° and 206° solar longitude, including the halo meteors (September 12 – October 19). The eccentricity is between 0.60 and 0.77, and between 0.45 and 0.92, including the halo meteors. The low number of meteors does not allow the maximum period to be defined; for guidance only we could say it happens around September 30 – October 1 (186° – 187° solar longitude). On this date the radiant is at RA = $20^{h}05^{m}$, Dec = +73°; about 3° from Epsilon Draconis.

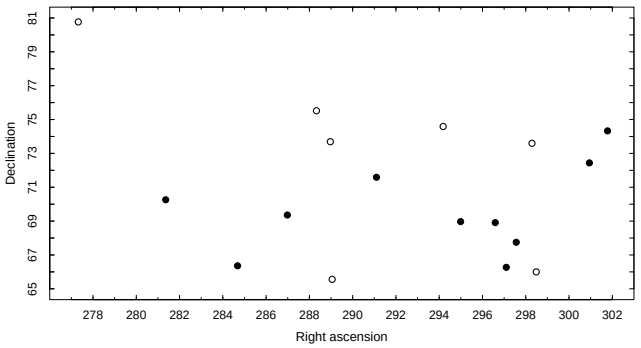

Figure 3 – Right Ascension and Declination of September epsilon Draconids. The open circles represent halo meteors of the shower and were not utilized in the present work.

Origin

Since all the meteors appear to have eccentricities between 0.60 and 0.80 and periods between 4 and 9 years, whose semi-major axes are between 2.5 and 4.25 AU, we can reasonably assume that the parent body is a comet belonging to the Jupiter family, or an asteroid coming from the nucleus of the no longer or only sporadically active family comet. Comparing the shower's average orbital elements with those of these comet families one can see no possible ancestor: the perihelia of these family comets, including those whose orbits tilt are between 40° and 50°, are very distant from Earth. The dispersion of meteoric orbits on about 15° of solar longitude (36°, including the halo meteors), and the high ratio of halo meteors and meteor shower (equal to about 0.58), suggests this shower to be an old one about to be scattered, originated from a no longer existing or now inactive comet parent body. The orbital elements of this shower have been compared with a selected set of asteroids whose orbits are comet-like (Fernandez, 2013); among these, (163732) 2003 KP2 has such orbital elements to suggest it could be a possible progenitor body, or a fragment of the progenitor body, of the shower (JPL, 2016). Today it is an asteroid with a diameter of around 3 km and a period of around 4.5 years, perhaps it is a dormant comet.

Periodicity

In the years 2009–2012 the shower appeared only in 2011; therefore we can say the shower is not annual but periodic. This would imply that its torus is not complete or is so rarefied that only thickening by gravitational perturbations can occasionally allow it to be observed. If the parent body was actually a comet belonging to the Jupiter comets – or even if it is not – its orbital elements, in particular the semi-major axis and eccentricities, make us believe that the shower is significantly perturbed by Jupiter (as happens to many other cometary showers whose outburst periods, every 11–12 years or multiple, are resonant with that of Jupiter). If this hypothesis is correct, the next significant activity of this shower, perhaps a mini outburst, should happen in 2022 or 2023. Similar activities could have happened in the past (1999–2000, 1987–1989, etc.). If (163732) 2003 KP2 is really its parent body it is possible that the next recordable activity occur in 2016, or more probably in 2020, the past activity might have occurred in 2007 or more probably in 2002.

Searches for previous observations

The Author looked for meteor showers features related to the current shower lists IAU [a], IMO [b] and the website

[a] http://meteor.asu.cas.cz/IAU/showerlist.pdf
[b] http://www.imonet.org/showers/index.html

Table 1 – Orbital elements of September epsilon Draconids and relative values of the criterion D_D with respect to the median value.

	#	Date and Time	$\lambda_\odot$	v_g	a	q	e	p	peri	node	incl	D_D
1	414	2009 09 19 210824	176.924	25.88	2.59	0.985	0.619967	4.176	198.08	176.92	42.82	0.0691
2	12805	2011 09 26 190027	183.181	26.11	3.18	0.980	0.692482	5.698	198.74	183.18	42.09	0.0191
3	12918	2011 09 27 191918	184.175	25.39	2.75	0.993	0.639518	4.574	192.44	184.17	41.67	0.0436
4	12922	2011 09 27 203237	184.225	26.54	4.25	0.981	0.769293	8.783	197.63	184.22	41.81	0.0588
5	13158	2011 09 30 013827	186.398	28.08	2.50	0.990	0.604513	3.965	193.99	186.39	47.38	0.0667
6	13357	2011 10 01 031704	187.448	30.15	3.48	0.985	0.717376	6.517	195.63	187.44	49.72	0.0382
7	13360	2011 10 01 032027	187.450	29.84	3.39	0.978	0.711952	6.261	199.17	187.45	49.10	0.0372
8	13374	2011 10 01 173401	188.033	27.98	2.97	0.979	0.670401	5.123	198.99	188.03	46.07	0.0244
9	13507	2011 10 02 195301	189.112	26.03	2.59	0.987	0.619958	4.188	195.37	189.11	43.09	0.0534
10	13702	2011 10 04 011730	190.318	25.62	4.17	0.993	0.76221	8.541	190.44	190.31	40.34	0.0602
11	13729	2011 10 04 023153	190.369	27.21	4.15	0.982	0.763615	8.477	196.56	190.36	43.21	0.0582
12	13768	2011 10 04 200710	191.090	26.09	3.03	0.994	0.672528	5.296	189.51	191.09	42.54	0.0279
Maximum difference of value				4.76	1.75	0.016	0.164780	4.818	9.66	14.17	9.38	0.0500
Minimum value				25.39	2.50	0.978	0.604513	3.965	189.51	176.92	40.34	0.0191
Medium value				27.08	3.25	0.986	0.686984	5.967	195.55	186.56	44.15	0.0464
Maximum value				30.15	4.25	0.994	0.769293	8.783	199.17	191.09	49.72	0.0691

Period from September 19 to October 4. Maximum September 30 - October 1 (?)

12007, 13211, 13626, 13691, 13930, 14315 and 528 are halo meteors (all are within the orbital elements range but they are excluded due to their large values of D_D).

	#	Date and Time	$\lambda_\odot$	v_g	a	q	e	p	peri	node	incl
A	12007	2011 09 13 031033	169.840	28.81	2.51	0.994	0.605007	3.998	194.10	169.84	48.96
B	13211	2011 09 30 174643	187.059	27.93	11.03	0.990	0.910257	36.666	192.47	187.05	42.57
C	13626	2011 10 03 213138	190.163	25.14	1.85	0.988	0.468	2.532	196.03	190.16	43.57
D	13691	2011 10 04 005346	190.302	28.28	1.81	0.993	0.453967	2.456	191.92	190.30	49.99
E	13930	2011 10 06 200745	193.061	28.29	13.52	0.977	0.927736	49.747	197.58	193.06	42.71
F	14315	2011 10 14 174737	200.869	26.20	2.54	0.982	0.613784	4.059	196.04	200.86	43.41
G	528	2009 10 18 214109	205.511	27.63	3.16	0.974	0.691419	5.617	198.60	205.51	44.91

Table 2 – Values of the criterion D_D reciprocal between pairs of September epsilon Draconids.

	414	12805	12918	12922	13158	13357	13360	13374	13507	13702	13729	13768
414	—	0.0651	0.0366	0.1143	0.0508	0.0962	0.0954	0.0724	0.0576	0.1207	0.1245	0.0755
12805	0.0651	—	0.0455	0.0528	0.0757	0.0491	0.0467	0.0368	0.0614	0.0605	0.0601	0.0409
12918	0.0366	0.0455	—	0.0946	0.0446	0.0768	0.0771	0.0510	0.0359	0.0927	0.0991	0.0405
12922	0.1143	0.0528	0.0946	—	0.1245	0.0576	0.0596	0.0761	0.1100	0.0326	0.0324	0.0753
13158	0.0508	0.0757	0.0446	0.1245	—	0.0869	0.0853	0.0574	0.0327	0.1238	0.1223	0.0644
13357	0.0962	0.0491	0.0768	0.0576	0.0869	—	0.0154	0.0426	0.0827	0.0650	0.0531	0.0575
13360	0.0954	0.0467	0.0771	0.0596	0.0853	0.0154	—	0.0350	0.0785	0.0689	0.0518	0.0585
13374	0.0724	0.0368	0.0510	0.0761	0.0574	0.0426	0.0350	—	0.0444	0.0783	0.0683	0.0380
13507	0.0576	0.0614	0.0359	0.1100	0.0327	0.0827	0.0785	0.0444	—	0.1055	0.1043	0.0448
13702	0.1207	0.0605	0.0927	0.0326	0.1238	0.0650	0.0689	0.0783	0.1055	—	0.0312	0.0638
13729	0.1245	0.0601	0.0991	0.0324	0.1223	0.0531	0.0518	0.0683	0.1043	0.0312	—	0.0690
13768	0.0755	0.0409	0.0405	0.0753	0.0644	0.0575	0.0585	0.0380	0.0448	0.0638	0.0690	—

of the Croatian Meteor Network[c], including showers not yet officially announced; but none were found.

4.2 43 Cassiopeiids (546 FTC)

The first people that mentioned this shower were Leonard Kornoš, Pavol Matlovič, Regina Rudawska, Juraj Tóth, Mária Hajduková, Jakub Koukal and Roman Piffl (Kornoš et al., 2014b). This shower comes from the study of 12 meteors, 11 belonging to the shower itself and one halo meteor. Orbital data of these meteors are shown in the Table 3: as pointed out above, the perihelion argument and inclination are included in an interval of less than 10° (Figures 4 and 5). The values of the 11 meteors subject to the Drummond criterion (D_D) are between 0.0474 and 0.1224, with a mean value of 0.0818 (Table 4). On the basis of only the data of the present work there is a possibility of 8.9% that the shower does not exist and was only a chance occurrence ($p = 0.089$). The geocentric coordinates of the radiant of the meteors are in the Figure 6.

Key Features

The period of visibility is between 136° and 156° of solar longitude, roughly corresponding to the period August

[c] http://cmn.rgn.hr/downloads/software/search-iau-mdc/streams.php

Table 3 – Orbital elements of the 43 Cassiopeiids and relative values of the criterion D_D.

#	Date and Time	$\lambda_\odot$	v_g	a	q	e	p	peri	node	incl	D_D
9375	2011 08 11 211623	138.701	52.82	7.32	1.009	0.862	19.81	172.44	138.70	97.20	0.0958
20728	2012 08 12 022339	139.615	51.30	11.08	1.007	0.909	36.91	171.31	139.61	92.29	0.0748
10310	2011 08 14 234322	141.677	55.43	−3.64	1.011	1.277	—	175.35	141.67	94.66	0.1224
10463	2011 08 16 200745	143.454	52.99	−6.65	1.005	1.151	—	170.95	143.45	91.26	0.0715
290	2009 08 16 222200	144.038	53.53	11.85	1.010	0.915	40.81	175.42	144.03	97.67	0.0573
20913	2012 08 16 214751	144.235	57.52	−3.76	1.006	1.268	—	171.81	144.23	99.95	0.1136
10645	2011 08 18 231541	145.502	51.27	12.67	1.007	0.920	45.15	172.29	145.50	91.88	0.0541
10772	2011 08 20 225201	147.411	53.69	15.43	1.002	0.935	60.62	168.77	147.41	97.56	0.0474
10845	2011 08 21 230003	148.379	52.27	7.24	1.005	0.861	19.50	170.59	148.37	95.61	0.0848
11007	2011 08 25 031234	151.439	55.86	−7.26	0.997	1.137	—	167.14	151.43	98.41	0.0832
11104	2011 08 29 001628	155.183	54.78	12.61	1.004	0.920	44.78	171.21	155.18	100.54	0.0946
Maximum difference of value			6.25		0.014	0.416		8.28	16.48	9.28	0.0749
Minimum value			51.27		0.997	0.861		167.14	138.70	91.26	0.0474
Medium value			53.77		1.006	1.014		171.57	145.42	96.09	0.0818
Maximum value			57.52		1.011	1.277		175.42	155.18	100.54	0.1224

Period from August 11 to 29. Maximum August 16 (?).

9246 and 10467 are halo meteors (9246 is within the orbital elements range but it is excluded due to its large value of D_D):

#	Date and Time	$\lambda_\odot$	v_g	a	q	e	p	peri	node	incl
9246	2011 08 11 010416	137.894	50.11	3.06	1.009	0.670	5.36	171.47	137.89	94.77
10467	2011 08 16 205846	143.488	52.59	12.48	0.996	0.920	44.15	165.25	143.48	95.21

Table 4 – Values of the criterion D_D reciprocal between pairs of 43 Cassiopeiids.

	9375	20728	10310	10463	290	20913	10645	10772	10845	11007	11104
9375	—	0.0389	0.1965	0.1515	0.0507	0.1968	0.0652	0.0798	0.0714	0.1742	0.1292
20728	0.0389	—	0.1715	0.1214	0.0500	0.1756	0.0445	0.0715	0.0742	0.1548	0.1291
10310	0.1965	0.1715	—	0.0645	0.1672	0.0481	0.1672	0.1689	0.2047	0.1236	0.2040
10463	0.1515	0.1214	0.0645	—	0.1226	0.0701	0.1131	0.1161	0.1519	0.0882	0.1577
290	0.0507	0.0500	0.1672	0.1226	—	0.1637	0.0375	0.0458	0.0522	0.1341	0.0907
20913	0.1968	0.1756	0.0481	0.0701	0.1637	—	0.1654	0.1551	0.1953	0.0902	0.1827
10645	0.0652	0.0445	0.1672	0.1131	0.0375	0.1654	—	0.0418	0.0464	0.1272	0.0912
10772	0.0798	0.0715	0.1689	0.1161	0.0458	0.1551	0.0418	—	0.0439	0.1036	0.0627
10845	0.0714	0.0742	0.2047	0.1519	0.0522	0.1953	0.0464	0.0439	—	0.1430	0.0679
11007	0.1742	0.1548	0.1236	0.0882	0.1341	0.0902	0.1272	0.1036	0.1430	—	0.1124
11104	0.1292	0.1291	0.2040	0.1577	0.0907	0.1827	0.0912	0.0627	0.0679	0.1124	—

11 to 29: in the years 2009–2012, the shower always appeared, except in 2010: we can therefore assume the shower is annual. The low number of meteors does not allow its maximum period to be specified. For guidance, it can be estimated to be around August 16 (143° – 144° solar longitude).

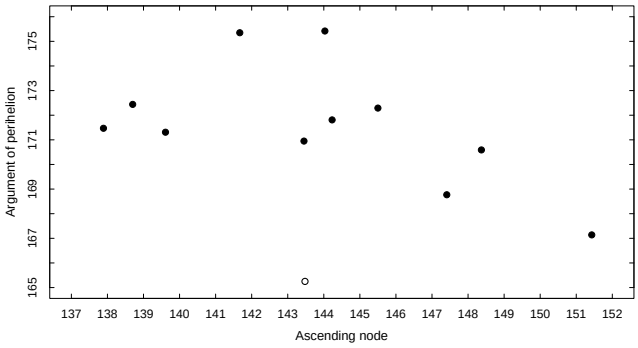

Figure 4 – The values of the ascending node and Argument of perihelion of 43 Cassiopeiids. The open circles represent halo meteors of the shower and were not utilized in the present work.

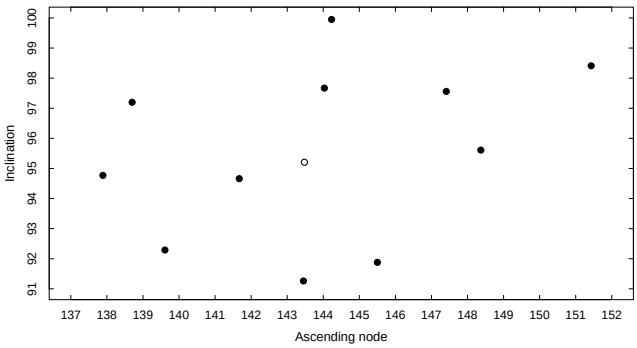

Figure 5 – The values of the ascending node and inclination of 43 Cassiopeiids. The open circles represent halo meteors of the shower and were not utilized in the present work.

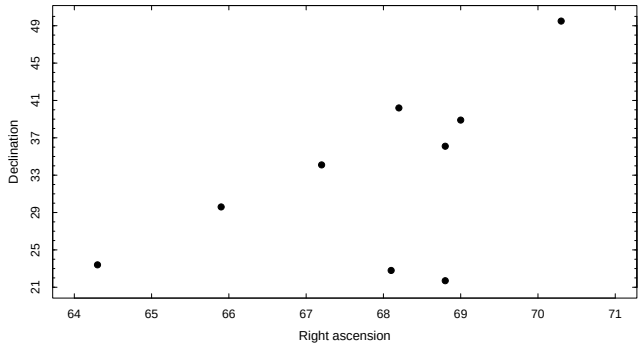

Figure 6 – Right Ascension and Declination of 43 Cassiopeids.

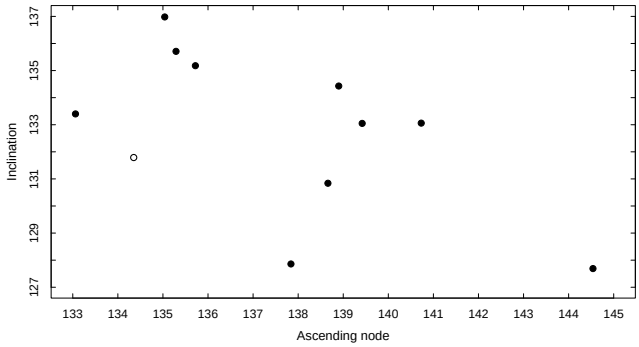

Figure 8 – The values of the ascending node and Inclination of kappa Perseids. The open circles represent halo meteors of the shower and were not utilized in the present work.

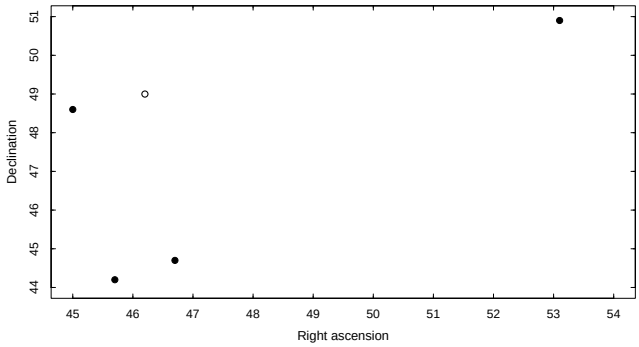

Figure 9 – Right Ascension and Declination of kappa Perseids. The open circles represent halo meteors of the shower and were not utilized in the present work.

Origin

Since all the meteors appear to have eccentricities greater than 0.800, it may be reasonably expected that the parent body is a comet rather than an asteroid: if the progenitor was actually a comet, its orbital elements, detected by more than half of the meteors, should suggest a comet of the Halley family. Comparison of the shower's average orbital elements with those of known comets did not yield any possible ancestor. The asteroid elements have not been examined. The dispersion of the meteoric orbits, almost perpendicular to the Earth's, on about 20° of solar longitude, suggests an old shower about to be scattered, and a parent body no longer existing or reduced to a dormant comet. If the parent body was actually a Halley type comet, we should expect a little outburst with a periodicity comparable to that of the comet; and we could also expected to find traces of these outbursts in the last 50–100 years archives.

4.3 kappa Perseids (547 KAP)

The first people that mentioned this shower were Leonard Kornoš, Pavol Matlovič, Regina Rudawska, Juraj Tóth, Mária Hajduková, Jakub Koukal and Roman Piffl (Kornoš et al., 2014b). This shower comes from the study of 10 meteors (there is too one halo meteor). Orbital data are shown in Table 5: as specified above the argument of perihelion and inclination are included in a less than 10° interval (Figures 7 and 8). The 10 meteors subjected to the Drummond criterion (D_D) have values between 0.0211 and 0.1265, with an average value of 0.0676. On the basis of only the data of the present work there is a possibility of 8.9% that the shower does not exist and was only a chance occurrence ($p = 0.089$) (Table 6). The geocentric coordinates of the radiant of the meteors are in the Figure 9.

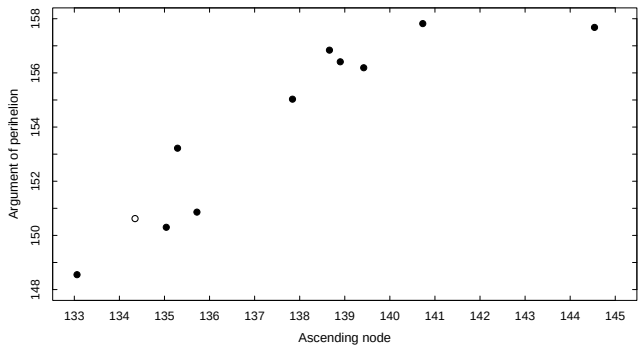

Figure 7 – The values of the ascending node and Argument of perihelion of kappa Perseids. The open circles represent halo meteors of the shower and were not utilized in the present work.

Key Features

The visibility period is between 133° and 145° of solar longitude, roughly corresponding to August 6–18: in the examined years (2009–2012), the shower appeared again with the exception of 2009 (the data collection began casually, just half the visibility period of this shower, in 2009); therefore we can assume that the shower is annual. The low number of meteors does not allow the determination of the maximum period; for example, it can be estimated around August 11–12 (138° – 139° solar longitude).

Origin

As nearly two-thirds of the meteor eccentricities are greater than 0.870, it may reasonably be expected that the parent body is a comet rather than an asteroid. The comparison between the shower's average orbital elements and those of known comets did not show any possible ancestor. Asteroidal elements were not examined. The dispersion of meteoric orbits on 11° of solar longitude, and the fact that almost two-thirds of the orbits are hyperbolic or high eccentric suggests a very long period – probably thousands of years – comet as

Table 5 – Orbital elements of kappa Perseids and relative values of the criterion D_D with respect to the medium value.

#	Date and Time	$\lambda_\odot$	v_g	a	q	e	p	peri	node	incl	D_D
8788	2011 08 06 000255	133.062	66.74	−5.786	0.934	1.161483	—	148.55	133.06	133.40	0.0912
8883	2011 08 08 013707	135.040	66.39	−23.513	0.946	1.04024	—	150.30	135.04	136.98	0.0419
2037	2010 08 08 014818	135.291	65.73	156.733	0.959	0.993876	1962.980	153.22	135.29	135.71	0.0211
20324	2012 08 08 010456	135.726	67.05	−6.541	0.945	1.144526	—	150.86	135.72	135.18	0.0805
9169	2011 08 10 234453	137.841	63.37	16.572	0.967	0.94161	67.495	155.03	137.84	127.86	0.0362
20536	2012 08 11 023124	138.660	64.89	−72.971	0.972	1.013326	—	156.84	138.66	130.84	0.0239
9569	2011 08 12 021805	138.902	63.13	4.089	0.976	0.761147	8.273	156.41	138.90	134.43	0.1265
20570	2012 08 11 213459	139.422	62.96	4.307	0.975	0.773485	8.944	156.19	139.42	133.05	0.1182
10070	2011 08 14 000715	140.733	63.97	7.348	0.978	0.866871	19.927	157.82	140.73	133.06	0.0640
10583	2011 08 17 232649	144.548	65.01	−9.697	0.972	1.100305	—	157.68	144.54	127.69	0.0723
Maximum difference of value			4.09		0.044	0.400336		9.27	11.48	9.29	0.1054
Minimum value			62.96		0.934	0.761147		148.55	133.06	127.69	0.0211
Medium value		137.922	64.92		0.962	0.979687		154.29	137.92	132.82	0.0676
Maximum value			67.05		0.978	1.161483		157.82	144.54	136.98	0.1265

Period from August 6 to 18. Maximum around August 11–12 (138°–139°)

1967 is a halo meteor (it is within the orbital elements range but it is excluded due to its large value of D_D):

#	Date and Time	$\lambda_\odot$	v_g	a	q	e	p	peri	node	incl
1967	2010 08 07 022844	134.359	69.12	−2.119	0.937	1.442194	—	150.62	134.35	131.79

Table 6 – Values of the criterion D_D reciprocal between pairs of kappa Perseids.

	8788	8883	2037	20324	9169	20536	9569	20570	10070	10583
8788	—	0.0622	0.0839	0.0239	0.1139	0.0822	0.2129	0.2052	0.1544	0.0752
8883	0.0622	—	0.0294	0.0489	0.0755	0.0475	0.1581	0.1512	0.0998	0.0732
2037	0.0839	0.0294	—	0.0727	0.0533	0.0333	0.1342	0.1271	0.0749	0.0804
20324	0.0239	0.0489	0.0727	—	0.1082	0.0720	0.2032	0.1957	0.1429	0.0631
9169	0.1139	0.0755	0.0533	0.1082	—	0.0422	0.1135	0.1036	0.0563	0.0878
20536	0.0822	0.0475	0.0333	0.0720	0.0422	—	0.1438	0.1351	0.0803	0.0568
9569	0.2129	0.1581	0.1342	0.2032	0.1135	0.1438	—	0.0116	0.0659	0.1880
20570	0.2052	0.1512	0.1271	0.1957	0.1036	0.1351	0.0116	—	0.0574	0.1787
10070	0.1544	0.0998	0.0749	0.1429	0.0563	0.0803	0.0659	0.0574	—	0.1243
10583	0.0752	0.0732	0.0804	0.0631	0.0878	0.0568	0.1880	0.1787	0.1243	—

the parent body. As an alternative to this hypothesis, it could be a Jovian family comet, no longer existing or not yet discovered.

5 Conclusions

The September epsilon Draconids are seen to be sufficiently distinctive to be considered as a new meteor shower, so far unknown to the scientific community. It is obviously essential for its existence to be confirmed by other researchers, through future observations and/or archive researches in databases. The availability of observations following the year 2012 provides an opportunity to verify the existence of the showers analysed here. The present work also confirms the existence of the 43 Cassiopeiids and kappa Perseids.

The limited number of meteors belonging to the three showers highlighted a particular kind of object called by the Author "halo meteor". These objects, previously observed and studied by many other researchers, are in the early stages of their transition from shower to sporadic meteor. Despite their similarities, each one of them is not obviously linked to any other and we are seeing the typical continuous dispersion of meteor showers. A table shows the D values of each meteor, compared to all the others in the same shower (Tables 2, 4 and 6). Such tables show the similarity between a given meteor and the others from the shower; and it also shows the trend of each single object to become a "halo meteor". This kind of table, if used with a huge number of meteors, can allow the identification of threads within a shower.

Acknowledgements

The Author thanks both Micaela Panella and Massimo Calabresi for the English translation, Tracie Heywood for improving the language, and also all the anonymous observers who patiently collected the data used for this work.

References

Fernandez Y. R. (2013). "Asteroids with comet-like orbits: Elements and positions". `http://www.physics.ucf.edu/~yfernandez/lowtj.html` .

Galligan D. P. (2001). "Performance of the D-criteria in recovery of meteoroid stream orbits in a radar data set". *Monthly Notices of the Royal Astronomical Society*, **327:2**, 623–628.

Jopek T. J. (2011). "Meteoroid streams and their parent bodies". *Memorie della Societa Astronomica Italiana*, **82**, 310–320.

JPL (2016). "163732 (2003 KP2)". `http://ssd.jpl.nasa.gov/sbdb.cgi?sstr=163732&orb=1` .

Klačka J. (2000). "Meteor stream membership criteria". *Astronomy and Astrophysics*. (`http://arxiv.org/pdf/astro-ph/0005509v1.pdf`, 25 May 2000).

Kornoš L., Koukal J., Piffl R., and Tóth J. (2014a). "EDMOND Meteor Database". In Gyssens M., Roggemans P., and Żołądek P., editors, *Proceedings of the International Meteor Conference, Poznań, Poland, Aug. 22-25, 2013*. International Meteor Organization, pages 23–25.

Kornoš L., Matlovič P., Rudawska R., Tóth J., Hajduková M. J., Koukal J., and Piffl R. (2014b). "Confirmation and characterization of IAU temporary meteor showers in EDMOND database". In Jopek T. J., Rietmeijer F. J. M., Watanabe J., and Williams I. P., editors, *Proceedings of the Meteoroids 2013 Conference Aug. 26-30, 2013, A.M. University, Poznań, Poland*. A.M. University Press, pages 225–233.

Langbroek M. (2007). "Some of my meteor related MS Excel applications". `http://marcolangbroek.tripod.com/metsoft.html` .

Welch P. G. (2001). "A new search method for streams in meteor data bases and its application". *Monthly Notices of the Royal Astronomical Society*, **328**, 101–111.

Handling Editor: Javor Kac

Preliminary results

Results of the IMO Video Meteor Network — February 2016

Sirko Molau[1], *Stefano Crivello*[2], *Rui Goncalves*[3], *Carlos Saraiva*[4], *Enrico Stomeo*[5], *and Javor Kac*[6]

The IMO Video Meteor Network cameras recorded more than 15 500 meteors in over 7 000 hours of observing time in 2016 February. The 2015 February 5 radar outburst of the γ-Lyrids cannot be detected in the video data. The 2015 January 9/10 radar outburst of the κ-Cancrids is confirmed. Video data enabled the calculation of the flux density profile which shows a sharp maximum on 2015 January 10 at 02^h50^m UT, with a FWHM of about 40 minutes.

Received 2016 July 11

1 Introduction

In Europe, February is not really renowned for pleasant weather, and 2016 was no exception in this respect. The lowlight was February 22/23, when 18 cameras recorded less than a hundred meteors in 64 hours of effective observing time. Many observers really had to be patient to get through the many clouded nights. Slovenia and Hungary experienced particularly poor conditions, whereas Portuguese and German observers were still relatively lucky. In addition we faced technical problems with computers (Hinwo1, Remo3), camera housings (Icc7) and software (Lic1, Lic2). In the end, only 16 out of 79 cameras managed to observe in twenty or more nights. With a total of 7 000 observing hours, the yield was comparable to 2012 and 2014, but far inferior to 2015. The same is true for those 15 500 meteors that we recorded (Table 2 and Figure 1).

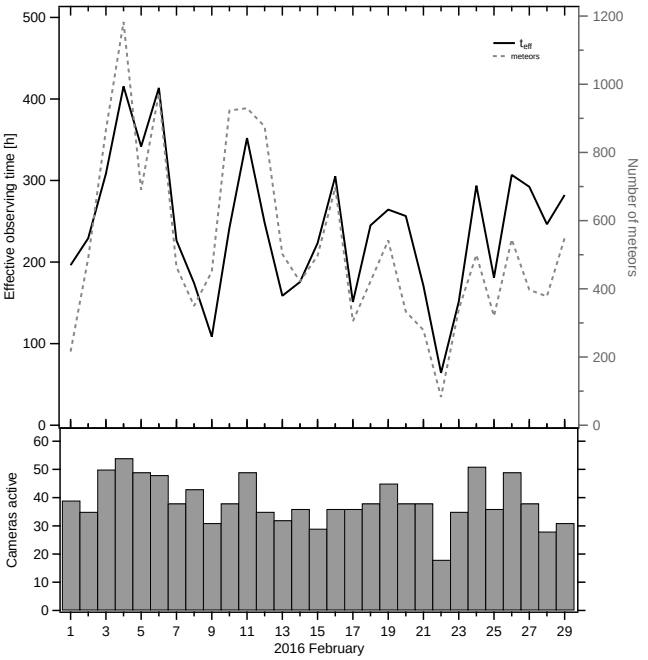

Figure 1 – Monthly summary for the effective observing time (solid black line), number of meteors (dashed gray line) and number of cameras active (bars) in 2016 February.

2 Confirming the 2015 radar outbursts of minor showers

2.1 γ-Lyrids

There are no signficant meteor showers in February – but still this month surprises us every now and then. We are neither talking about the Chelyabinsk meteorite fall of February 2013, nor of the meteorite fall in Copenhagen this year. We rather refer to the outbursts of hitherto unknown meteor showers that Peter Brown reported about at the 2016 IMC (Brown, 2016). His search for unusual activity spikes in the 2013–2016 Canadian CMOR radar data was successful twice. On 2015 February 5, CMOR discovered the γ-Lyrids (794 GLY) which stood out almost 20 sigma from the background. On previous occasions we learned that some meteor showers detected by CMOR are invisible in the optical domain because they consist of very small particles, but we also had successful confirmations. So it was worthwhile to check the data of the IMO Video Meteor Network. Our long-term analysis based on a million meteors recorded until 2011 (Molau, 2014) showed not a single radiant which resembled the radar data. Also a re-calculation of the shower membership of the observations on 2015 February 4 and 5 revealed just a few chance alignments. The subsequent radiant search did not yield any similar radiant at all. So we can safely assume that the γ-Lyrids are either another radar meteor shower, or that the peak fell exactly into the European daytime hours.

2.2 κ-Cancrids of January

The second event reported by Brown (2016) occurred only a few days earlier on 2015 January 9/10. This time the signal of the wavelet analysis was 17 sigma above

[1]Abenstalstr. 13b, 84072 Seysdorf, Germany.
Email: sirko@molau.de
[2]Via Bobbio 9a/18, 16137 Genova, Italy.
Email: stefano.crivello@libero.it
[3]Urbanizacao da Boavista, Lote 46, Linhaceira, 2305-114 Asseiceira, Tomar, Portugal. Email: rui.goncalves@ipt.pt
[4]Rua Aquilino Ribeiro, 23 - 1 Dto. 2790028 Carnaxide, Portugal. Email: carlos.saraiva@netcabo.pt
[5]via Umbria 21/d, 30037 Scorze (VE), Italy.
Email: stom@iol.it
[6]Na Ajdov hrib 24, 2310 Slovenska Bistrica, Slovenia.
Email: javor.kac@orion-drustvo.si

IMO bibcode WGN-444-molau-vidfeb
NASA-ADS bibcode 2016JIMO...44..116M

Table 1 – Individual radiants of the κ-Cancrids, derived from IMO video observations between 1999 and 2011. Rk is the rank of the radiant. The last row gives the figures that Peter Brown (2016) derived from CMOR radar data.

$\lambda_\odot$	α	δ	v_{geo}	Rk
287°	138.°3	13.°5	50	46
288°	141.°6	12.°0	46	27
289°	138.°7	7.°5	50	5
290°	138.°2	7.°5	49	5
291°	136.°9	6.°5	42	22
292°	139.°5	8.°5	48	5
293°	144.°2	7.°5	48	8
294°	144.°2	7.°5	48	11
289.°5	137.°8	8.°9	47.°3	—

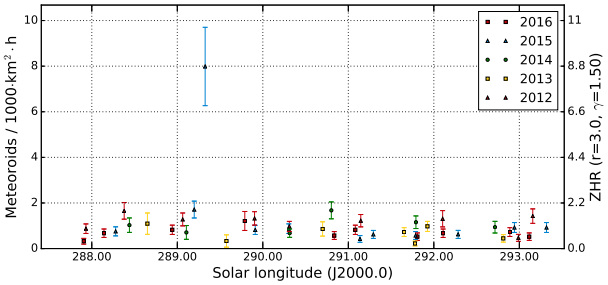

Figure 2 – Flux density of the κ-Cancrids in the years 2012–2016, derived from observations of the IMO Network.

the mean background level. The κ-Cancrids (793 KCA) peaked just one week after the Quadrantids, and this time the search in our video data was more fruitful. We found a first sign of activity in our long-term analysis at 287° and 288° solar longitude. Between $\lambda_\odot = 289°$ and 292° the shower was clearly detected – with a rank of five it was one of the strongest sources in the sky by that time. At solar longitude 293° and 294° it disappeared again. Since the activity interval is relatively short and the shower was hardly detected at 291° solar longitude, we did not recognize it in our previous shower search.

Details about the radiants are given in Table 1. They prove that the κ-Cancrids were not active in 2015 for the first time, but already before 2012. That is consistent with the observations of Peter Brown, since the radar data also showed a weak annual component beside the strong outburst in 2015.

Finally, we re-calculated the meteor shower assignments for the years 2012–2016 in the solar longitude interval in question. This was to check if the outburst of 2015 was also visible in the optical domain, or if it consisted of minor particles only. The result is given in Figure 2. Whereas the κ-Cancrids hardly stand out from the sporadic background in all other intervals, they were well detected on 2015 January 9/10, with a flux density of 8 meteoroids per 1 000 km^2 per hour.

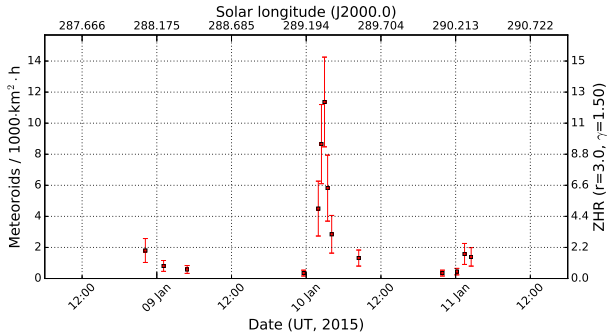

Figure 3 – High resolution activity profile of the κ-Cancrids in 2015, derived from observations of the IMO Network.

To refine the peak time, the video data of 2015 were analysed once more with a higher resolution (Figure 3). The minimum bin size was 30 minutes, whereby each bin needed to contain at least five shower members or 10 000 km^2 and hour of normalized collection area. Luckily, the peak fell exactly into the European nighttime hours – in this resolution we can discern both the ascending and descending activity branch. Based on roughly 50 shower meteors which were recorded by all video cameras together in the night of question, we determined peak activity at 2015 January 10 at 02^h50^m UT, corresponding to 289.°315 solar longitude. The full width at half maximum (FWHM) of the peak was only about 40 minutes.

And how strong was the outburst? Our video data yield a factor of ten compared to other years and observing intervals. Two things have to be considered when interpreting the 17 sigma of CMOR: On the one hand, that was obtained relative to the background. In the year before, the κ-Cancrids were also detected several sigma above the background, as otherwise the annual component would not have been visible. In this respect, the increase was less than a factor of ten. On the other hand, the temporal resolution of the CMOR wavelet analysis was lower than in the video data, which smeared out the narrow peak. Hence, the factor of ten should be of the right order.

References

Brown P. (2016). "Recent Canadian Meteor Orbit Radar (CMOR) detected meteor shower outbursts". In Roggemans A. and Roggemans P., editors, *Proceedings of the International Meteor Conference, Egmond, the Netherlands, 2–5 June 2016*. IMO, pages 42–45.

Molau S. (2014). "Meteor showers identified from one million video meteors". In Gyssens M., Roggemans P., and Zoladek P., editors, *Proceedings of the International Meteor Conference, Poznan, Poland, 22-25 August 2013*. pages 26–38.

Handling Editor: Javor Kac

Code	Name	Location	Camera	FOV [°²]	Stellar LM [mag]	Eff.CA [km²]	Nights	Time [h]	Meteors
ARLRA	Arlt	Ludwigsfelde/DE	Ludwig2 (0.8/8)	1475	6.2	3779	20	107.4	427
BANPE	Bánfalvi	Zalaegerszeg/HU	Huvcse01 (0.95/5)	2423	3.4	361	4	3.6	23
BERER	Berkó	Ludányhalászi/HU	Hulud1 (0.8/3.8)	5542	4.8	3847	1	1.6	10
BOMMA	Bombardini	Faenza/IT	Mario (1.2/4.0)	5794	3.3	739	14	92.9	248
BREMA	Breukers	Hengelo/NL	Mbb3 (0.75/6)	2399	4.2	699	18	161.9	205
BRIBE	Klemt	Herne/DE	Hermine (0.8/6)	2374	4.2	678	21	145.4	202
		Bergisch Gladbach/DE	Klemoi (0.8/6)	2286	4.6	1080	19	101.8	118
CASFL	Castellani	Monte Baldo/IT	Bmh1 (0.8/6)	2350	5.0	1611	17	134.8	283
			Bmh2 (1.5/4.5)*	4243	3.0	371	17	106.9	187
CRIST	Crivello	Valbrevenna/IT	Bilbo (0.8/3.8)	5458	4.2	1772	17	92.6	236
			C3P8 (0.8/3.8)	5455	4.2	1586	16	91.1	171
			Stg38 (0.8/3.8)	5614	4.4	2007	17	105.0	387
DONJE	Donani	Faenza/IT	Jenni (1.2/4)	5886	3.9	1222	12	59.8	217
ELTMA	Eltri	Venezia/IT	Met38 (0.8/3.8)	5631	4.3	2151	9	55.2	106
FORKE	Förster	Carlsfeld/DE	Akm3 (0.75/6)	2375	5.1	2154	10	67.2	140
GONRU	Goncalves	Tomar/PT	Templar1 (0.8/6)	2179	5.3	1842	24	174.8	438
			Templar2 (0.8/6)	2080	5.0	1508	22	170.0	345
			Templar3 (0.8/8)	1438	4.3	571	18	155.6	142
			Templar4 (0.8/3.8)	4475	3.0	442	23	156.9	316
			Templar5 (0.75/6)	2312	5.0	2259	24	163.3	367
GOVMI	Govedič	Središče ob Dravi/SI	Orion2 (0.8/8)	1447	5.5	1841	9	46.7	68
			Orion3 (0.95/5)	2665	4.9	2069	10	57.5	90
			Orion4 (0.95/5)	2662	4.3	1043	12	62.4	70
HERCA	Hergenrother	Tucson/US	Salsa3 (0.8/3.8)	2336	4.1	544	29	286.7	438
IGAAN	Igaz	Hódmezővásárhely/HU	Huhod (0.8/3.8)	5502	3.4	764	16	81.1	116
		Budapest/HU	Hupol (1.2/4)	3790	3.3	475	10	63.5	17
JONKA	Jonas	Budapest/HU	Husor (0.95/4)	2286	3.9	445	2	3.9	2
			Husor2 (0.95/3.5)	2465	3.9	715	15	78.8	74
KACJA	Kac	Ljubljana/SI	Orion1 (0.8/8)	1399	3.8	268	4	19.2	10
		Kamnik/SI	Cvetka (0.8/3.8)*	4914	4.3	1842	6	24.3	36
			Rezika (0.8/6)	2270	4.4	840	6	27.0	98
			Stefka (0.8/3.8)	5471	2.8	379	5	23.5	30
KOSDE	Koschny	Izana Obs./ES	Icc7 (0.85/25)*	714	5.9	1464	4	25.0	138
			Lic1 (2.8/50)*	2255	6.2	5670	11	62.9	550
		La Palma/ES	Icc9 (0.85/25)*	683	6.7	2951	24	173.3	1413
			Lic2 (3.2/50)*	2199	6.5	7512	12	106.2	1084
		Noordwijkerhout/NL	Lic4 (1.4/50)*	2027	6.0	4509	7	28.8	18
LOJTO	Łojek	Grabniak/PL	Pav57 (1.0/5)	1631	3.5	269	9	48.1	79
LOPAL	Lopes	Lisbon/PT	Naso1 (0.75/6)	2377	3.8	506	17	138.9	74

Table 2 – Observers contributing to 2016 February data of the IMO Video Meteor Network. Eff.CA designates the effective collection area; the overall number of nights is the number of nights with at least one camera operating, the overall observing time and number of meteors are sums over all cameras.

Table 2 – Observers contributing to 2016 February data of the IMO Video Meteor Network – continued from previous page.

Code	Name	Location	Camera	FOV [°²]	Stellar LM [mag]	Eff.CA [km²]	Nights	Time [h]	Meteors
MACMA	Maciejewski	Chełm/PL	Pav35 (0.8/3.8)	5495	4.0	1584	14	96.0	160
			Pav36 (0.8/3.8)*	5668	4.0	1573	16	83.5	127
			Pav43 (0.75/4.5)*	3132	3.1	319	13	86.2	67
			Pav60 (0.75/4.5)	2250	3.1	281	16	93.3	161
MARGR	Maravelias	Lofoupoli-Crete/GR	Loomecon (0.8/12)	738	6.3	2698	16	92.7	133
MARRU	Marques	Lisbon/PT	Ran1 (1.4/4.5)	4405	4.0	1241	16	131.2	163
MASMI	Maslov	Novosibirsk/RU	Nowatec (0.8/3.8)	5574	3.6	773	11	54.9	109
MOLSI	Molau	Seysdorf/DE	Avis2 (1.4/50)*	1230	6.9	6152	9	55.3	142
			Escimo2 (0.85/25)	155	8.1	3415	7	56.3	24
			Mincam1 (0.8/8)	1477	4.9	1084	22	101.7	215
		Ketzür/DE	Remo1 (0.8/8)	1467	6.5	5491	21	123.8	467
			Remo2 (0.8/8)	1478	6.4	4778	24	130.8	439
			Remo3 (0.8/8)	1420	5.6	1967	3	8.6	10
			Remo4 (0.8/8)	1478	6.5	5358	23	133.7	434
MORJO	Morvai	Fülöpszállás/HU	Huful (1.4/5)	2522	3.5	532	19	134.3	109
MOSFA	Moschini	Rovereto/IT	Rover (1.4/4.5)	3896	4.2	1292	16	12.6	79
OCHPA	Ochner	Albiano/IT	Albiano (1.2/4.5)	2944	3.5	358	2	15.6	15
OTTMI	Otte	Pearl City/US	Orie1 (1.4/5.7)	3837	3.8	460	14	75.2	83
PERZS	Perkó	Becsehely/HU	Hubec (0.8/3.8)*	5498	2.9	460	13	89.4	225
ROTEC	Rothenberg	Berlin/DE	Armefa (0.8/6)	2366	4.5	911	9	48.2	36
SARAN	Saraiva	Carnaxide/PT	Ro1 (0.75/6)	2362	3.7	381	16	131.2	172
			Ro2 (0.75/6)	2381	3.8	459	19	159.7	229
			Ro3 (0.8/12)	710	5.2	619	19	169.1	281
			Sofia (0.8/12)	738	5.3	907	17	148.0	185
SCALE	Scarpa	Alberoni/IT	Leo (1.2/4.5)*	4152	4.5	2052	8	38.4	47
SCHHA	Schremmer	Niederkrüchten/DE	Doraemon (0.8/3.8)	4900	3.0	409	18	125.0	164
SLAST	Slavec	Ljubljana/SI	Kayak1 (1.8/28)	563	6.2	1294	7	36.9	102
			Kayak2 (0.8/12)	741	5.5	920	7	45.8	42
STOEN	Stomeo	Scorze/IT	Min38 (0.8/3.8)	5566	4.8	3270	17	74.3	259
			Noa38 (0.8/3.8)	5609	4.2	1911	19	85.3	261
			Sco38 (0.8/3.8)	5598	4.8	3306	16	89.3	353
STRJO	Strunk	Herford/DE	Mincam2 (0.8/6)	2354	5.4	2751	24	133.1	310
			Mincam3 (0.8/6)	2338	5.5	3590	20	118.9	198
			Mincam4 (1.0/2.6)	9791	2.7	552	14	68.2	89
			Mincam5 (0.8/6)	2349	5.0	1896	20	127.1	162
			Mincam6 (0.8/6)	2395	5.1	2178	23	135.1	185
TEPIS	Tepliczky	Agostyán/HU	Huago (0.75/4.5)	2427	4.4	1036	13	70.0	78
			Humob (0.8/6)	2388	4.8	1607	12	77.0	122
TRIMI	Triglav	Velenje/SI	Sraka (0.8/6)*	2222	4.0	546	12	34.9	75
YRJIL	Yrjölä	Kuusankoski/FI	Finexcam (0.8/6)	2337	5.5	3574	7	28.6	41
* active field of view smaller than video frame						Overall	29	7 024.9	15 526

Results of the IMO Video Meteor Network — March 2016, and discussion about the meteor limiting magnitude

Sirko Molau[1], *Stefano Crivello*[2], *Rui Goncalves*[3], *Carlos Saraiva*[4], *Enrico Stomeo*[5], *and Javor Kac*[6]

In 2016 March, the IMO Video Meteor Network cameras recorded almost 18 000 meteors in over 8 000 hours of observing time. An observing summary is presented. A procedure for meteor limiting magnitude calculation is discussed and plans for MetRec revision presented.

Received 2016 July 24

1 Introduction

In 2016 March, the weather situation improved a little when compared to 2016 February. In particular in the first half of the month we obtained longer observation series, whereas the conditions started to deteriorate again in the second half. The highest number of cameras was active on March 17 and 26 (61 of 78 cameras). Since we were spoiled with over 10 000 observing hours in the last two years, we fell significantly short of this result with only 8 300 hours in 2016 (Table 1 and Figure 1). However, the average hourly meteor count was higher than before, in particular thanks to the image-intensified cameras of Detlef Koschny on the Canary Islands. So the overall outcome of nearly 18 000 meteors was still respectable. 29 cameras managed to observe in twenty or more nights, which is a clear increase compared to 2016 February. On the other hand, there were hardly any cameras with less than ten nights, which hints at geographically-balanced observing conditions. Only Portugal and Tucson/US deviated significantly from the average. Indeed Carl Hergenrother missed only two nights in the first quarter of 2016 with his camera Salsa3, which is another proof for the excellence of his observing site.

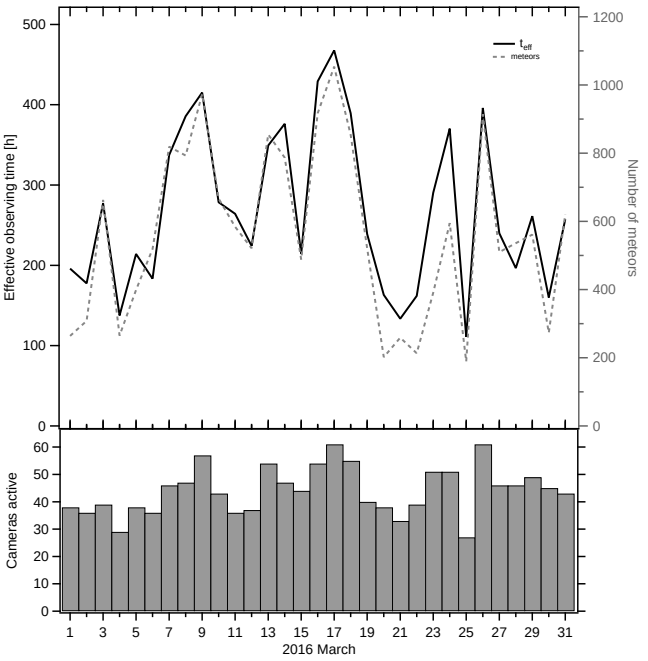

Figure 1 – Monthly summary for the effective observing time (solid black line), number of meteors (dashed gray line) and number of cameras active (bars) in 2016 March.

2 MetRec and meteor magnitude

Since March cannot present noticeable meteor shower activity, we want to address a technical issue in this report, inspired by a presentation at the Meteoroids 2016 conference (Kingery et al., 2016). It is about the difference between stellar and meteor limiting magnitude (lm) and the dependency from the angular meteor velocity. This difference plays a central role in the flux density determination. At first, the stellar lm is calculated every minute. Then the expected angular velocity of a shower meteor is determined for every pixel in the field of view. Based on this, the stellar magnitude is converted into a meteor limiting magnitude, the effective collection area for the meteor shower is computed, and finally the flux density is determined.

It is obvious that, due to the motion, the photons of a meteor are spread out over more CCD pixels than the photons of a star. The faster the meteor moves, the fewer photons remain per pixel and the smaller is the meteor limiting magnitude. For punctiform objects, the loss is inversely proportional to the angular velocity. However, stars and meteors are not punctiform objects in practice, but have a certain size on a CCD. A formula was obtained for MetRec many years ago, based on the simplified assumption that all pixels have the same brightness. The formula consists of three segments: If the meteor is moving less than its own diameter within one video frame, there is no loss in limiting magnitude. If the meteor is moving fast enough, the above-mentioned inverse proportionality is valid, inbetween there is a transition phase. This function depends on the minimum diameter of stars. However, in practice a constant minimum diameter was applied to all cameras, since otherwise the results varied too much between the cameras.

[1]Abenstalstr. 13b, 84072 Seysdorf, Germany.
Email: sirko@molau.de
[2]Via Bobbio 9a/18, 16137 Genova, Italy.
Email: stefano.crivello@libero.it
[3]Urbanizacao da Boavista, Lote 46, Linhaceira, 2305-114 Asseiceira, Tomar, Portugal. Email: rui.goncalves@ipt.pt
[4]Rua Aquilino Ribeiro, 23 - 1 Dto. 2790028 Carnaxide, Portugal. Email: carlos.saraiva@netcabo.pt
[5]via Umbria 21/d, 30037 Scorze (VE), Italy.
Email: stom@iol.it
[6]Na Ajdov hrib 24, 2310 Slovenska Bistrica, Slovenia.
Email: javor.kac@orion-drustvo.si

IMO bibcode WGN-444-molau-vidmar
NASA-ADS bibcode 2016JIMO...44..120M

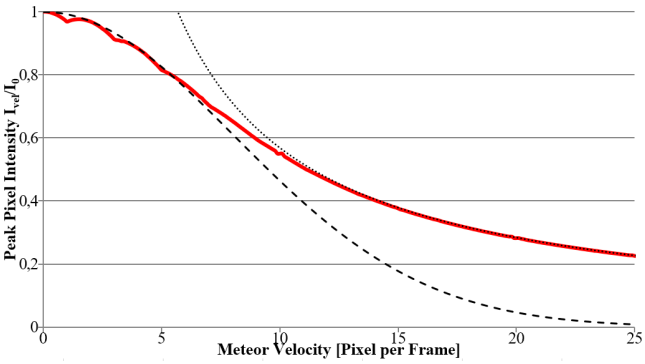

Figure 2 – Decrease of the maximum intensity of a pixel depending on the angular velocity (solid line). Dashed line represents a Gaussian function and dotted line a CONST/velocity type of function.

At the Meteoroids conference, A. Kingery and R. Blaauw (2016) presented their method to calculate the meteor limiting magnitude of a video camera. The approach is comparable to MetRec, even though the stellar limiting magnitude is calculated only every ten minutes and deviates slightly from the star field counting method of MetRec. Thereafter a transformation is applied to derive the loss in limiting magnitude, which is inversely proportional to the angular velocity. They go one step further by modelling stars and meteors with a two-dimensional Gaussian as Point Spread Function (PSF). The full width at half maximum (FWHM) is one parameter in their formula, but CCD pixels are still modelled as punctiform. That was the trigger for a more detailed analysis, what the dependency really looks like.

At first, the loss in limiting magnitude was modelled in software. It was based on a star with a radial-symmetric two-dimensional Gaussian PSF and predefined variance. Another assumption was a linear response of the CCD chip, i.e. that twice as many photons would generate a signal twice as strong. To save computation time, the star was discretized with 10 times the resolution of a CCD pixel. Then it was calculated in very small time steps how the star is moving during the exposure of a video frame parallel to the x-axis, and how the pixels accumulate the photons (in reality the meteor is moving, not the star, but for simplicity we talk about simulating a star trail here). The velocity of the stellar motion was the second parameter of the simulation. At the end of the "exposure", both the pixel sum over the full CCD chip (which was independent of the velocity as expected) and the brightest individual pixel were calculated. The ratio of that pixel value and the brightest pixel at velocity zero was finally the searched loss in intensity I_v/I_0 and represents the loss in limiting magnitude as a function of velocity v.

Figure 2 shows the simulation result for a star with a variance of 5 pixels and a velocity between 0 and 25 pixels / frame. We can see that at velocities close to zero the dependency is Gaussian shaped, and at high velocities it can be modelled by a function of type CONST/velocity. In-between there is a transition area that cannot be modelled by either of these functions. Thus, the three phases of the original MetRec model are confirmed. Furthermore, the simulation helped to derive a better functional approximation.

As remarked earlier, the limiting magnitude is governed by the pixel which receives most photons during the exposure. From simple considerations we conclude that it is the pixel at the center of the star trail. But how many photons does that pixel receive during the exposure? If the star is not moving, it is always the peak of the Gaussian curve that exposes the pixel (Figure 3, left). If the star is moving slowly, the integral from slightly right to slightly left of the Gaussian is calculated (Figure 3, center). The faster the star moves, the larger will be the integral over the Gaussian curve, i.e. also the remote areas with small values are summed up (Figure 3, right). The integral is divided by the velocity, since the time that the Gaussian is spending on each pixel is getting ever shorter. That is, we are looking for the mean of the Gaussian function from right to left of the peak.

Naturally the mean is getting smaller, the more remote areas of the Gaussian are included, as is depicted schematically in Figure 4. If only the inner section is considered, the mean is identical to the peak of the Gaussian. The more areas are included, the smaller the mean gets.

Depending on the velocity v, the mean can be calculated by determining the integral over the Gaussian curve $g(x)$ (from $-v/2$ to $+v/2$) and dividing it by the length of the segment (v). The integral of a Gaussian is related to Gaussian error function $\mathrm{erf}(x)$. That is a sigmoid function (Figure 5) with a value of -1 at $x = -\infty$, 0 at $x = 0$, and $+1$ at $x = +\infty$.

Depending on the variance σ^2, the antiderivative $G(x)$ is

$$G(x) = \frac{1}{2}\left(1 + \mathrm{erf}\left(\frac{x}{\sqrt{2\,\sigma^2}}\right)\right) \tag{1}$$

To calculate the integral, we have to subtract the antiderivative at $x = -v/2$ from the antiderivative at $x = v/2$. Since $\mathrm{erf}(x) = -\mathrm{erf}(-x)$ we can simplify the difference to

$$G\left(\frac{v}{2}\right) - G\left(-\frac{v}{2}\right) = \mathrm{erf}\left(\frac{-v}{2\sqrt{2\,\sigma^2}}\right) \tag{2}$$

That value has to be divided by the velocity, because we want to calculate the average value of the Gauss function in the interval from $-v/2$ to $+v/2$. Hence we obtain the mean value by

$$g_v = \frac{\mathrm{erf}\left(\frac{-v}{2\sqrt{2\,\sigma^2}}\right)}{v} \tag{3}$$

Finally we have to scale this function, since it shall yield a value of 1.0 for $v \to 0$ (i.e. no loss in limiting magnitude when the star is not moving). The peak value of the Gauss function at $x = 0$ depends on the variance and can be expressed by $g(0) = 1/\sqrt{2\pi\,\sigma^2}$. So we have to divide the mean function (3) by this factor to obtain the dependency of the maximum pixel value

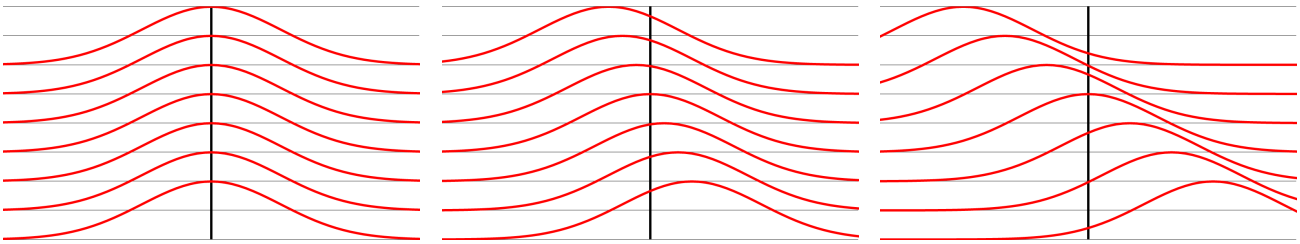

Figure 3 – Exemplary presentation of the motion of a star over the CCD pixel with maximum intensity (black line). If the star is not moving (left), always the peak of the Gaussian is accumulated. The faster the star moves (center, right), the more remote areas of the Gaussian curve are covered.

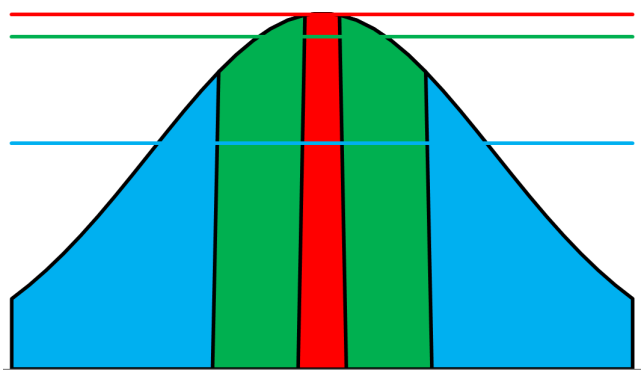

Figure 4 – The wider the considered part of the Gaussian (marked in color), the smaller gets the mean (horizontal lines).

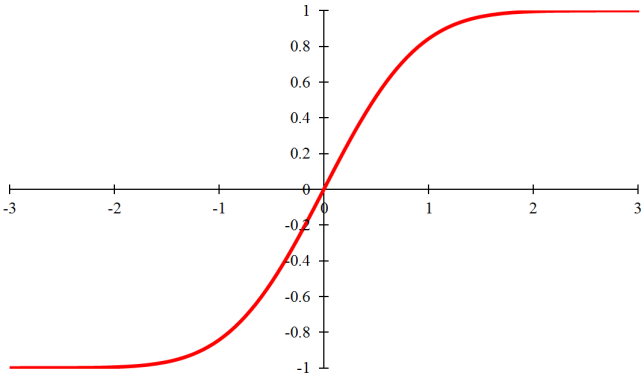

Figure 5 – The Gaussian error function $\mathrm{erf}(x)$ is a sigmoid function.

(resp. intensity) I_v relative to the maximum pixel value at velocity zero I_0

$$I_v/I_0 = \sqrt{2\pi\,\sigma^2} \cdot \mathrm{erf}\left(\frac{v}{2\sqrt{2\,\sigma^2}}\right)/v \qquad (4)$$

Figure 6 confirms that the loss in intensity obtained from the computer simulation can be approximated well by formula (4). The function is not defined for $v = 0$ (division by zero), but that does not matter because for $v = 0$ the ratio is unity by definition. To transform the loss in intensity I_v/I_0 into a loss of limiting magnitude $lm_v - lm_0$, we have to regard the logarithmic dependency between intensity I and limiting magnitude lm as $lm \sim 2.5\log_{10}(I)$. Thus

$$lm_v - lm_0 = -2.5\log_{10}(I_v/I_0) \qquad (5)$$

Two arbitrary examples: For a variance of 2 pixels and a velocity of 5 pixels / frame we obtain an intensity

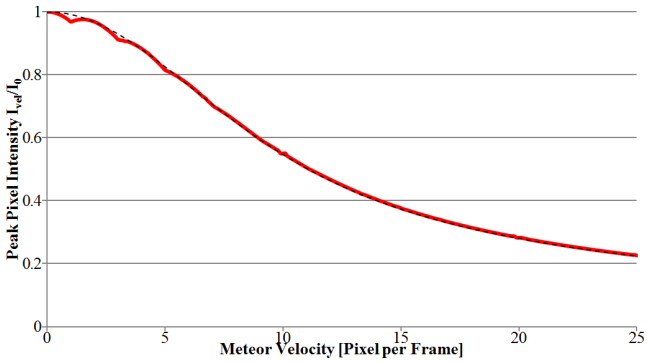

Figure 6 – Decrease of the maximum intensity of a pixel depending on the angular velocity (solid line). The dashed line represents the corresponding model according to formula (4).

Figure 7 – Simulated star trails for different variances (from 1 in the first to 10 in the last row) and velocities (from 0 in the first to 50 in the last column).

ratio I_v/I_0 of 0.65. That is, the maximum intensity is reduced by about 1/3 and the loss in limiting magnitude $lm_v - lm_0$ is −0.46 mag. Given a variance of 5 pixels and a velocity of 3 pixels / frame, we get $I_v/I_0 = 0.93$ and $lm_v - lm_0 = 0.08$ mag.

Next we repeated the simulation for Gaussian PSFs with different variances. Figure 7 shows different simulated star trails. The variance (1 to 10 pixels) is displayed in the vertical direction, and the velocities (0 to 50 pixels / frame) in the horizontal direction.

Figure 8 compared the intensity loss obtained from simulation with the model of formula (4). On the left side, the absolute values are given, on the right side the deviations between simulation and model. We see some numerical effects of the simulation (fluctuation at multiples of 10 pixels / frame) and two new effects. On the one hand, the intensity loss is slightly overestimated for all velocities, which becomes particularly obvious at the smallest variance value $\sigma^2 = 0.5$. On the other hand, the ratio oscillates at very small velocities and variances.

Both effects can be attributed to the fact that CCD pixels are punctiform in the model, but have a certain

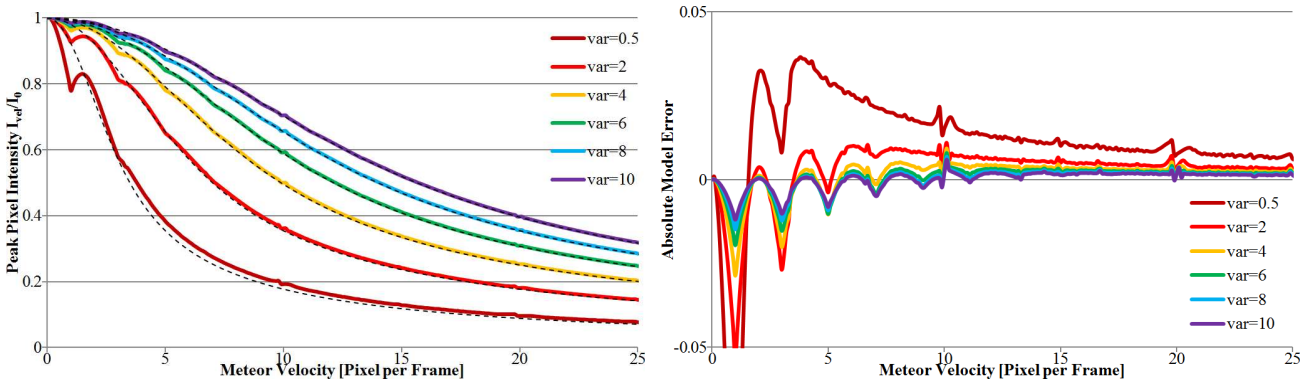

Figure 8 – Decrease of the maximum intensity of a pixel depending on the angular velocity (solid line) for Gaussian PSFs with different variances (left). Dashed lines show the corresponding model according to formula (4). On the right side, the deviation between simulation and model is shown.

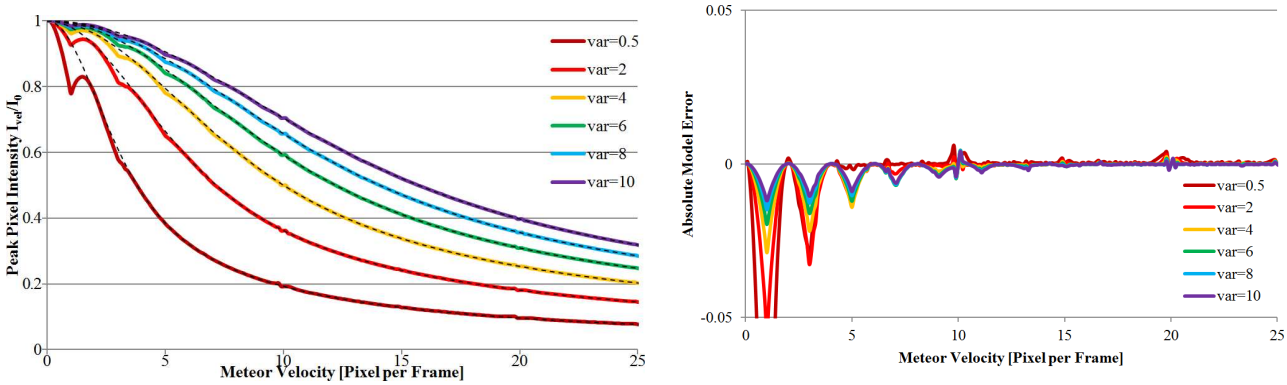

Figure 9 – Decrease of the maximum intensity of a pixel depending on the angular velocity (solid line) for Gaussian PSFs with different variances (left). Dashed lines show the corresponding model according to formula (6). On the right side, the deviation between simulation and model is shown.

size in reality (and in the simulation). This discretization has two effects:

- Even if the exposure time is reduced arbitrarily towards zero, each CCD pixel does not obtain exactly one brightness value from the Gaussian curve, but rather a small integral of the Gaussian of the size of a CCD pixel. That happens in both dimensions (x- and y-axis). A precise numerical solution may be possible but it is complex and not really necessary, as the systematic error is very small. This integration effect is kind of "smearing out" the Gaussian a bit. In result we obtain a function that resembles a Gaussian with slightly larger variance. It was found empirically that a small offset of 0.09 added to the variance in formula (4) removes the systematic deviation almost completely (Figure 9).

- The strong oscillation at small variances and velocities are a kind of aliasing. The root cause is that the pixel with maximum intensity at the center of the star trail is not changing continuously, but only in certain discrete steps due to the extend of the CCD pixels. On some occasions, the peak of photons is collected by exactly one pixel, at slightly higher velocities it is shared between two neighboring pixels, and once more at slightly higher velocities it is concentrated in one pixel again. The sum over all pixels of the star trail remains unchanged, but for the limiting magnitudes only the one pixel with maximum intensity is relevant.

Such an aliasing can be observed in other situations as well. If, for example, a thin black line is scanned, which is almost parallel to one axis, then the brightness of the line is oscillating between black and grey, because sometimes the light is focused on one pixel and sometimes it is shared between two pixels. The effect can also be measured, if an almost punctiform star moves almost exactly along one CCD line and the light is alternating shared between one or two pixels.

It is important that the exact position and size of these oscillations depends on where the simulation is started. In the simulation presented above, the center of the Gaussian function was located directly above the first pixel at start. If this start value is modified by a fraction of a pixel in x and/or y direction, both the shape and location of the oscillations change, but otherwise the graph remains the same. Since the variations are damped significantly at larger variances and velocities and even an error in the ratio by 0.1 yields only about a tenth of a magnitude, this oscillation can be ignored.

In result we obtain the final best approximation for the loss in intensity I_v/I_0 depending on the variance and velocity:

$$I_v/I_0 = \sqrt{2\pi(\sigma^2+0.09)} \cdot \frac{\operatorname{erf}\left(\frac{v}{2\sqrt{2(\sigma^2+0.09)}}\right)}{v} \qquad (6)$$

In the near future, MetRec will be adapted as follows: At first, the average variance of star images is determined for the video camera. Based on that, the loss in limiting magnitude is calculated based on formulae (5) and (6), whereby the variance is given in pixels and the velocity in pixels / frame. Strictly speaking, the formulae are valid only under the above-mentioned boundary conditions (radial-symmetric Gaussian as PSF, linear response of CCD), but it is independent of the background illumination, for example. The signal of the star has to be a certain amount above the background, but the absolute value of the background is irrelevant.

Note that T. Ott and E. Drolshagen presented a model at the IMC 2016, how the exact position of start and end point of a shutter break can be modelled by a function that depends on the Gaussian error function $\operatorname{erf}(x)$ as well (Ott et al., 2016). In fact, the simulation software used here has to be adapted only slightly to confirm also their model by simulation. It will be interesting to see, which effects the discretization of the CCD pixel and a variable brightness along the star trail has. That will be part of a future analysis.

References

Kingery A., Blaauw R., and Cooke W. J. (2016). "Determination of the meteor limiting magnitude". In *Meteoroids 2016 Conference, Noordwijk, the Netherlands, 6–10 June 2016*.

Ott T., Drolshagen E., Koschny D., and Poppe B. (2016). "PaDe - The particle detection program". In Roggemans A. and Roggemans P., editors, *Proceedings of the International Meteor Conference, Egmond, the Netherlands, 2–5 June 2016*. International Meteor Organization, pages 209–213.

Handling Editor: Javor Kac

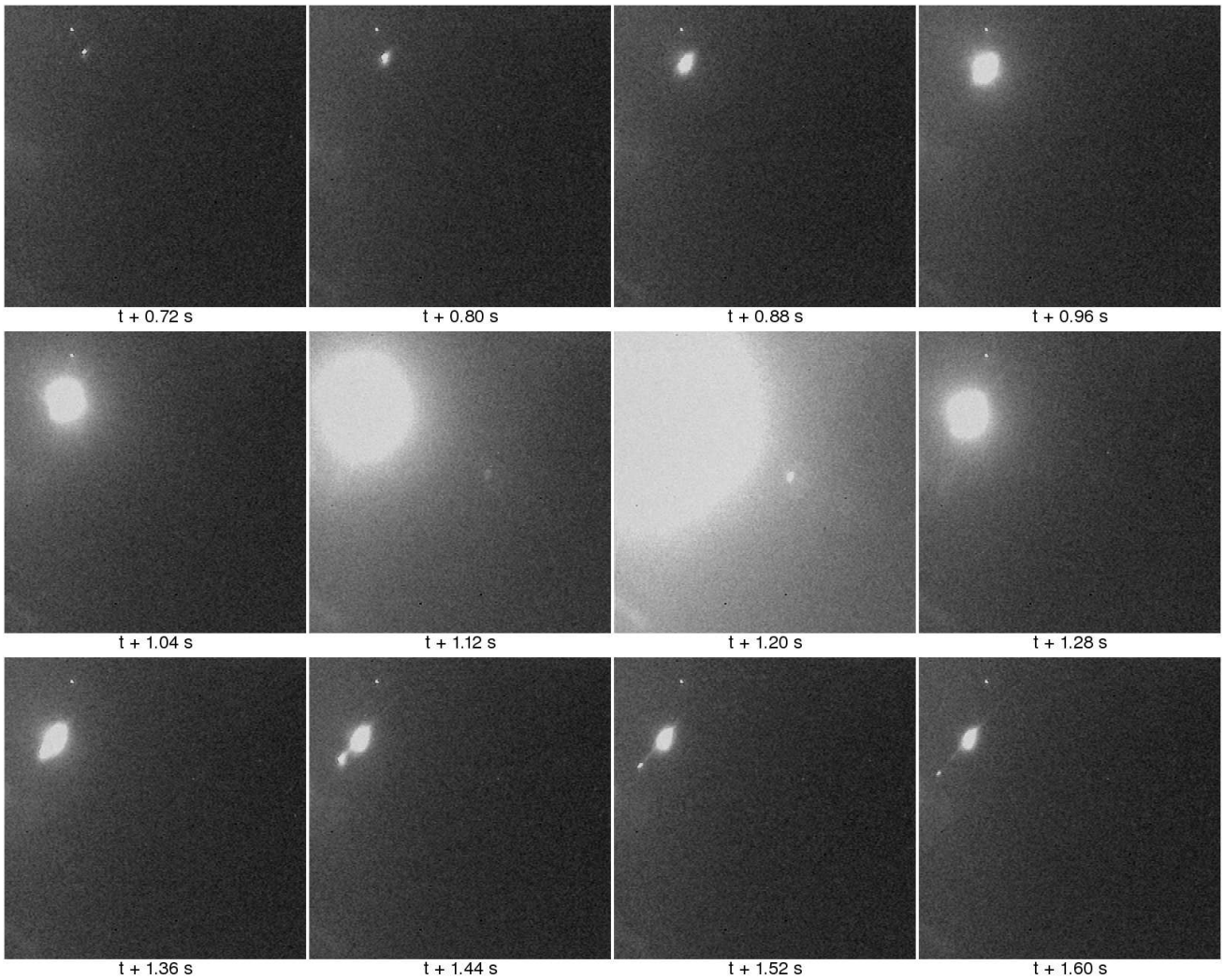

– Individual frames of a −10 magnitude sporadic meteor, recorded by Stefka camera on 2016 March 18 at $02^{\mathrm{h}}42^{\mathrm{m}}58^{\mathrm{s}}$ UT. Frames are marked with time since the beginning of the fireball. Note that persistent train glowed with at least magnitude −5 shortly after the fireball. Image courtesy: Javor Kac.

Code	Name	Location	Camera	FOV [°²]	Stellar LM [mag]	Eff.CA [km²]	Nights	Time [h]	Meteors
ARLRA	Arlt	Ludwigsfelde/DE	Ludwig2 (0.8/8)	1475	6.2	3779	19	85.6	317
BANPE	Bánfalvi	Zalaegerszeg/HU	Huvcse01 (0.95/5)	2423	3.4	361	7	4.0	26
BERER	Berkó	Ludányhalászi/HU	Hulud1 (0.8/3.8)	5542	4.8	3847	10	22.9	152
BOMMA	Bombardini	Faenza/IT	Mario (1.2/4.0)	5794	3.3	739	19	103.7	214
BREMA	Breukers	Hengelo/NL	Mbb3 (0.75/6)	2399	4.2	699	20	136.4	154
BRIBE	Klemt	Herne/DE	Hermine (0.8/6)	2374	4.2	678	11	79.8	140
		Bergisch Gladbach/DE	Klemoi (0.8/6)	2286	4.6	1080	15	112.9	139
CASFL	Castellani	Monte Baldo/IT	Bmh1 (0.8/6)	2350	5.0	1611	19	138.0	231
			Bmh2 (1.5/4.5)*	4243	3.0	371	19	126.4	205
CRIST	Crivello	Valbrevenna/IT	Bilbo (0.8/3.8)	5458	4.2	1772	24	147.8	276
			C3P8 (0.8/3.8)	5455	4.2	1586	21	109.5	165
			Stg38 (0.8/3.8)	5614	4.4	2007	24	170.2	530
DONJE	Donani	Faenza/IT	Jenni (1.2/4)	5886	3.9	1222	19	100.2	259
ELTMA	Eltri	Venezia/IT	Met38 (0.8/3.8)	5631	4.3	2151	11	51.1	81
FORKE	Förster	Carlsfeld/DE	Akm3 (0.75/6)	2375	5.1	2154	11	58.0	111
GONRU	Goncalves	Tomar/PT	Templar1 (0.8/6)	2179	5.3	1842	27	207.5	460
			Templar2 (0.8/6)	2080	5.0	1508	27	218.1	400
			Templar3 (0.8/8)	1438	4.3	571	24	192.9	138
			Templar4 (0.8/3.8)	4475	3.0	442	28	198.7	305
			Templar5 (0.75/6)	2312	5.0	2259	26	183.3	312
GOVMI	Govedič	Središče ob Dravi/SI	Orion2 (0.8/8)	1447	5.5	1841	10	51.5	85
			Orion3 (0.95/5)	2665	4.9	2069	10	47.2	46
			Orion4 (0.95/5)	2662	4.3	1043	9	44.3	41
HERCA	Hergenrother	Tucson/US	Salsa3 (0.8/3.8)	2336	4.1	544	30	288.1	375
IGAAN	Igaz	Hódmezővásárhely/HU	Huhod (0.8/3.8)	5502	3.4	764	20	72.0	78
		Budapest/HU	Hupol (1.2/4)	3790	3.3	475	9	52.3	13
JONKA	Jonas	Budapest/HU	Husor (0.95/4)	2286	3.9	445	18	109.1	61
			Husor2 (0.95/3.5)	2465	3.9	715	19	96.2	79
KACJA	Kac	Ljubljana/SI	Orion1 (0.8/8)	1399	3.8	268	15	82.8	79
		Kamnik/SI	Cvetka (0.8/3.8)*	4914	4.3	1842	7	54.6	136
			Rezika (0.8/6)	2270	4.4	840	6	45.0	137
			Stefka (0.8/3.8)	5471	2.8	379	6	52.1	87
KOSDE	Koschny	Izana Obs./ES	Icc7 (0.85/25)*	714	5.9	1464	22	163.1	807
			Lic1 (2.8/50)*	2255	6.2	5670	22	136.7	1029
		La Palma/ES	Icc9 (0.85/25)*	683	6.7	2951	24	190.0	1522
			Lic2 (3.2/50)*	2199	6.5	7512	23	178.6	1446
		Noordwijkerhout/NL	Lic4 (1.4/50)*	2027	6.0	4509	15	95.9	67
LOJTO	Łojek	Grabniak/PL	Pav57 (1.0/5)	1631	3.5	269	7	49.7	81
LOPAL	Lopes	Lisbon/PT	Naso1 (0.75/6)	2377	3.8	506	23	150.4	92

Table 1 – Observers contributing to 2016 March data of the IMO Video Meteor Network. Eff.CA designates the effective collection area; the overall number of nights is the number of nights with at least one camera operating, the overall observing time and number of meteors are sums over all cameras.

Table 1 – Observers contributing to 2016 March data of the IMO Video Meteor Network – continued from previous page.

Code	Name	Location	Camera	FOV [°²]	Stellar LM [mag]	Eff.CA [km²]	Nights	Time [h]	Meteors
MACMA	Maciejewski	Chełm/PL	Pav35 (0.8/3.8)	5495	4.0	1584	15	86.8	201
			Pav36 (0.8/3.8)*	5668	4.0	1573	17	81.0	128
			Pav43 (0.75/4.5)*	3132	3.1	319	13	81.7	64
			Pav60 (0.75/4.5)	2250	3.1	281	15	77.1	159
MARGR	Maravelias	Lofoupoli-Crete/GR	Loomecon (0.8/12)	738	6.3	2698	14	106.5	115
MARRU	Marques	Lisbon/PT	Cab1 (0.8/3.8)	5291	3.1	467	18	123.7	172
			Ran1 (1.4/4.5)	4405	4.0	1241	19	161.6	159
MASMI	Maslov	Novosibirsk/RU	Nowatec (0.8/3.8)	5574	3.6	773	9	33.5	131
MOLSI	Molau	Seysdorf/DE	Avis2 (1.4/50)*	1230	6.9	6152	23	127.1	448
			Escimo2 (0.85/25)	155	8.1	3415	15	77.9	159
			Mincam1 (0.8/8)	1477	4.9	1084	17	99.9	210
		Ketzür/DE	Remo1 (0.8/8)	1467	6.5	5491	21	114.7	379
			Remo2 (0.8/8)	1478	6.4	4778	23	123.0	367
			Remo3 (0.8/8)	1420	5.6	1967	11	47.8	84
			Remo4 (0.8/8)	1478	6.5	5358	19	121.7	364
MORJO	Morvai	Fülöpszállás/HU	Huful (1.4/5)	2522	3.5	532	22	144.8	75
MOSFA	Moschini	Rovereto/IT	Rover (1.4/4.5)	3896	4.2	1292	14	9.4	56
OTTMI	Otte	Pearl City/US	Orie1 (1.4/5.7)	3837	3.8	460	14	26.0	65
PERZS	Perkó	Becsehely/HU	Hubec (0.8/3.8)*	5498	2.9	460	18	81.5	175
SARAN	Saraiva	Carnaxide/PT	Ro1 (0.75/6)	2362	3.7	381	22	145.1	168
			Ro2 (0.75/6)	2381	3.8	459	21	166.3	204
			Ro3 (0.8/12)	710	5.2	619	22	169.2	249
			Sofia (0.8/12)	738	5.3	907	19	145.9	151
SCALE	Scarpa	Alberoni/IT	Leo (1.2/4.5)*	4152	4.5	2052	19	72.6	76
SCHHA	Schremmer	Niederkrüchten/DE	Doraemon (0.8/3.8)	4900	3.0	409	20	136.0	164
SLAST	Slavec	Ljubljana/SI	Kayak1 (1.8/28)	563	6.2	1294	14	63.2	83
			Kayak2 (0.8/12)	741	5.5	920	12	84.4	50
STOEN	Stomeo	Scorze/IT	Min38 (0.8/3.8)	5566	4.8	3270	24	85.0	202
			Noa38 (0.8/3.8)	5609	4.2	1911	24	106.4	223
			Sco38 (0.8/3.8)	5598	4.8	3306	21	100.9	282
STRJO	Strunk	Herford/DE	Mincam2 (0.8/6)	2354	5.4	2751	19	110.3	301
			Mincam3 (0.8/6)	2338	5.5	3590	16	103.1	158
			Mincam4 (1.0/2.6)	9791	2.7	552	16	83.0	88
			Mincam5 (0.8/6)	2349	5.0	1896	17	102.6	146
			Mincam6 (0.8/6)	2395	5.1	2178	15	97.7	128
TEPIS	Tepliczky	Agostyán/HU	Huago (0.75/4.5)	2427	4.4	1036	20	128.2	113
			Humob (0.8/6)	2388	4.8	1607	21	131.7	153
TRIMI	Triglav	Velenje/SI	Sraka (0.8/6)*	2222	4.0	546	13	43.3	48
YRJIL	Yrjölä	Kuusankoski/FI	Finexcam (0.8/6)	2337	5.5	3574	18	89.6	141
* active field of view smaller than video frame						Overall	31	8 296.8	17 515

The International Meteor Organization

web site http://www.imo.net

Council

President: Cis Verbeeck,
Bogaertsheide 5, 2560 Kessel, Belgium.
e-mail: cis.verbeeck@scarlet.be

Vice-President: Jürgen Rendtel,
Eschenweg 16, D-14476 Marquardt, Germany.
tel. +49 33208 50753
e-mail: jrendtel@aip.de

Secretary-General: Robert Lunsford,
1828 Cobblecreek Street, Chula Vista,
CA 91913-3917, USA. tel. +1 619 585 9642
e-mail: lunro.imo.usa@cox.net

Treasurer: Marc Gyssens, Heerbaan 74,
B-2530 Boechout, Belgium.
e-mail: marc.gyssens@uhasselt.be
BIC: GEBABEBB
IBAN: BE30 0014 7327 5911
Always state BIC and IBAN codes together!
Check international transfer charges with your bank; you are responsible for paying these.

Other Council members:

Megan Argo, Jodrell Bank Centre for Astrophysics, Alan Turing building, University of Manchester, Oxford Road, Manchester, M13 9PL, UK.
e-mail: megan.argo@gmail.com

Geert Barentsen, NASA Ames Research Center, M/S 244-30, Moffett Field CA 94035, USA.
e-mail: hello@geert.io

Javor Kac (see details under WGN)

Detlef Koschny, Zeestraat 46,
NL-2211 XH Noordwijkerhout, Netherlands.
e-mail: detlef.koschny@esa.int

Masahiro Koseki, 4-3-5 Annaka, Annaka-shi,
Gunma-ken 379-0116, Japan.
e-mail: geh04301@nifty.ne.jp

Sirko Molau, Abenstalstraße 13b, D-84072 Seysdorf, Germany. e-mail: sirko@molau.de

Jean-Louis Rault, Société Astronomique de France, 16, rue de la Vallée, 91360 Epinay sur Orge, France. e-mail: f6agr@orange.fr

Paul Roggemans, Pijnboomstraat 25, 2800 Mechelen, Belgium, e-mail: paul.roggemans@gmail.com

Galina Ryabova, Research Institute of Applied Mathematics and Mechanics of Tomsk State University, Lenin pr. 36, build. 27, 634050 Tomsk, Russian Federation.
e-mail: ryabova@niipmm.tsu.ru

Damir Šegon, J. Rakovca 3, 52100 Pula, Croatia. e-mail: damir.segon@pu.t-com.hr

Juraj Tóth, Faculty of Mathematics, Physics and Informatics, Comenius University in Bratislava, Mlynska dolina, 84248 Bratislava, Slovakia.
e-mail: toth@fmph.uniba.sk

Commission Directors

Visual Commission: Rainer Arlt (rarlt@aip.de)
Generic e-mail address: visual@imo.net
Electronic visual report form:
http://www.imo.net/visual/report/electronic

Video Commission: Sirko Molau (sirko@molau.de)
Generic e-mail address: video@imo.net

Photographic Commission: Bill Ward (William.Ward@glasgow.ac.uk)
Generic e-mail address: photo@imo.net

Radio Commission: Jean-Louis Rault (f6agr@orange.fr)
Generic e-mail address: radio@imo.net

Fireballs: Online fireball reports:
http://fireballs.imo.net

Outreach Officer

Jure Atanackov, e-mail: jureatanackov@gmail.com

Press Officer

Megan Argo, e-mail: megan.argo@gmail.com

WGN

Editor-in-chief: Javor Kac
Na Ajdov hrib 24, SI-2310 Slovenska Bistrica, Slovenia. e-mail: wgn@imo.net;
include METEOR in the e-mail subject line

Editorial board: Ž. Andreić, M. Argo, D.J. Asher, J. Correira, M. Gyssens, C. Hergenrother, T. Heywood, J. Rendtel, J.-L. Rault, C. Verbeeck.

IMO Sales

Available from the Treasurer or the Electronic Shop on the IMO Website	€	$
IMO membership, including subscription to WGN Vol. 44 (2016)		
Surface mail	26	39
Air Mail (outside Europe only)	49	69
Electronic subscription only	21	29
Back issues of WGN on paper (price per complete volume)		
Vols. 26 (1998) – 35 (2007)	15	23
Vols. 37 (2009) – 43 (2015) – electronic version only	9	13
Proceedings of the International Meteor Conference on paper		
1990, 1991, 1993, 1995, 1996, 1999, 2000, 2002, 2003, per year	9	13
2007, 2010, 2011, per year	15	23
2012, 2013, 2014, 2015 per year	25	37
Proceedings of the Meteor Orbit Determination Workshop 2006	15	23
Radio Meteor School Proceedings 2005	15	23
Handbook for Meteor Observers	15	23
Meteor Shower Workbook	12	18
Electronic media		
Meteor Beliefs Project CD-ROM	6	9
DVD: WGN Vols. 6–30 & IMC 1991, 1993–96, 2001–04	45	69

Perseid fireball of 2016 August 12 from Slovenia

This bright Perseid fireball of estimated magnitude −8 appeared over Slovenia on 2016 August 12, at $01^{\mathrm{h}}48^{\mathrm{m}}02^{\mathrm{s}}$ UT and was witnessed by many observers being out that night.

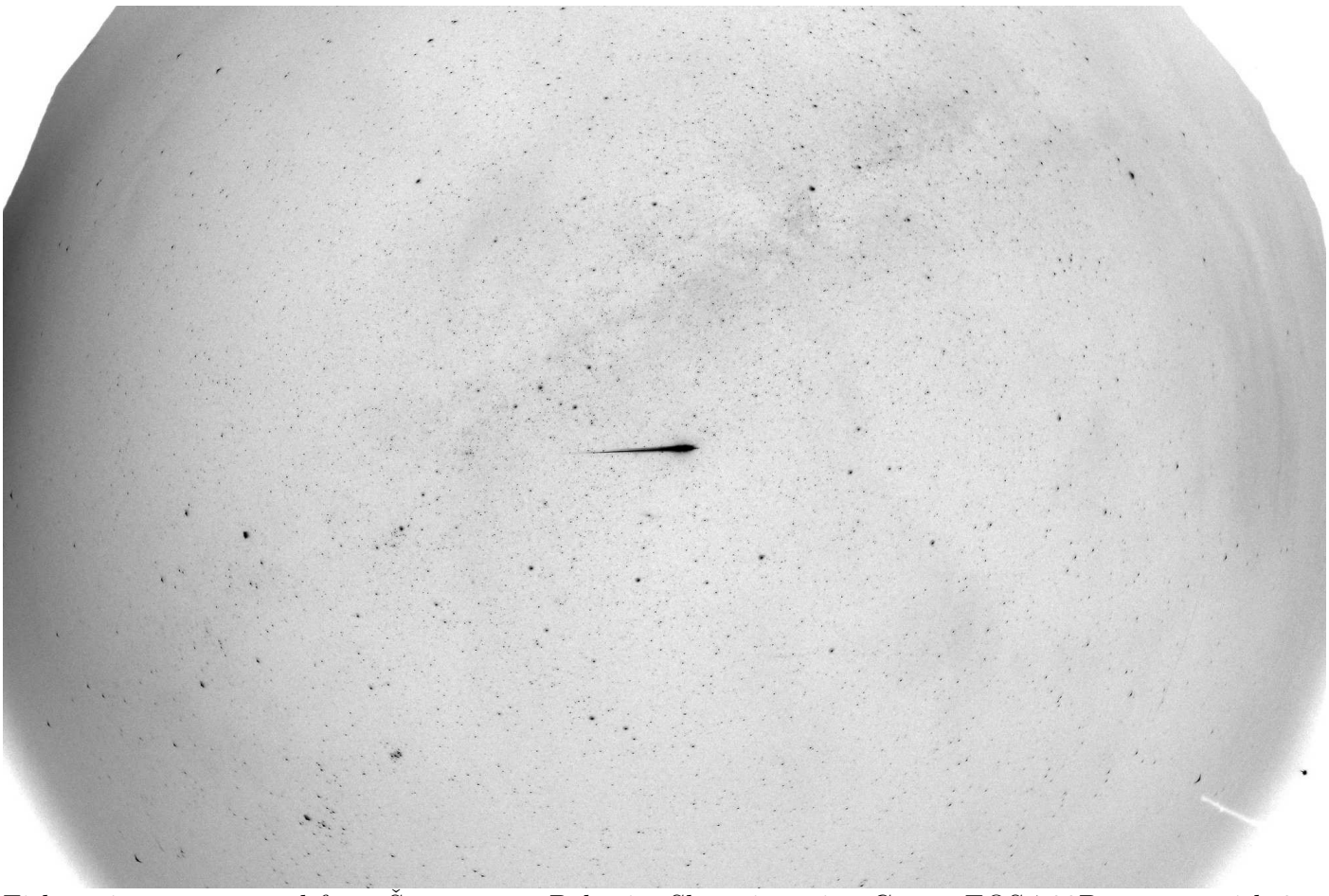

Fisheye image captured from Šmartno na Pohorju, Slovenia, using Canon EOS 700D camera with 8-mm $f/3.5$ lens and 30 s exposure at ISO 3200. Image courtesy: Igor Žiberna.

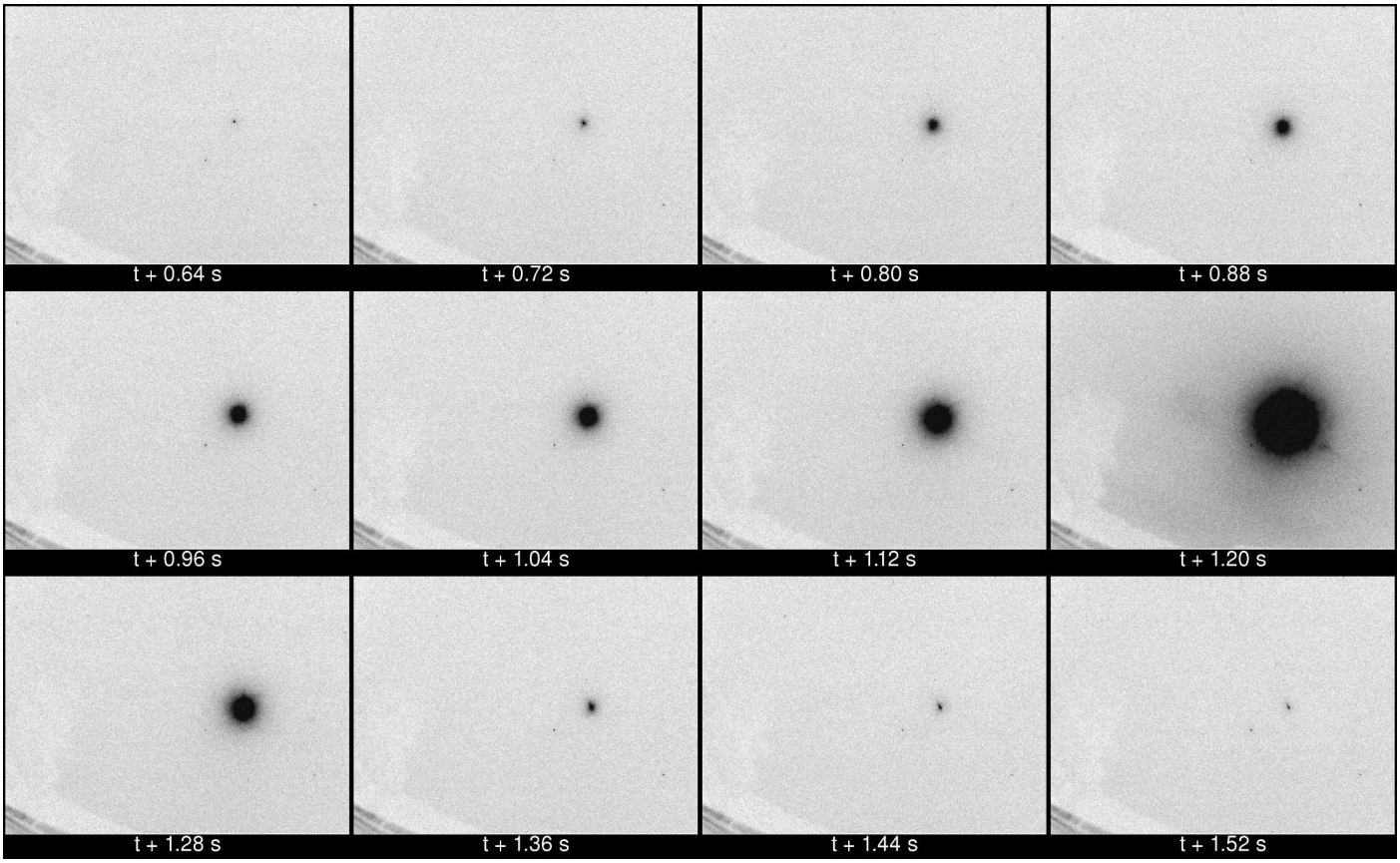

Still frames from video recording made by Cvetka camera stationed at Rezman Observatory, Slovenia, using 3.8-mm $f/0.8$ lens. Frames are marked with time since the beginning of the fireball. Image courtesy: Javor Kac.